A DISSERTATION FOR THE DEGREE OF DOCTOR OF PHILOSOPHY

Molecular Analysis of Cell Death Induced by Autoactive Pepper Nucleotide-binding Leucine-rich Repeat Genes

고추의 자가활성 Nucleotide-binding Leucine-rich Repeat 유전자가 유도하는 세포사멸기작 연구

FEBRUARY 2019

HYE-YOUNG LEE

MAJOR IN HORTICULTURAL SCIENCE AND BIOTECHNOLOGY

DEPARTMENT OF PLANT SCIENCE

COLLEGE OF AGRICULTURE AND LIFE SCIENCES

THE GRADUATE SCHOOL OF SEOUL NATIONAL UNIVERSITY

Molecular Analysis of Cell Death Induced by Autoactive Pepper Nucleotide-binding Leucine-rich Repeat Genes

UNDER THE DIRECTION OF DR. DOIL CHOI
SUBMITTED TO THE FACULTY OF THE GRADUATE SCHOOL OF
SEOUL NATIONAL UNIVERSITY

BY
HYE-YOUNG LEE

MAJOR IN HORTICULTURAL SCIENCE AND BIOTECHNOLOGY
DEPARTMENT OF PLANT SCIENCE

FEBRUARY 2019

APPROVED AS A QUALIFIED DISSERTATION OF HYE-YOUNG LEE
FOR THE DEGREE OF DOCTOR OF PHILOSOPHY
BY THE COMMITTEE MEMBERS

CHAIRMAN	**Byoung-Cheorl Kang, Ph.D.**
VICE-CHAIRMAN	**Doil Choi, Ph.D.**
MEMBER	**Jeong Mee Park, Ph.D.**
MEMBER	**Ji-Joon Song, Ph.D.**
MEMBER	**Cecile Segonzac, Ph.D.**

Molecular Analysis of Cell Death Induced by Autoactive Pepper Nucleotide-binding Leucine-rich Repeat Genes

Hye-Young Lee

Department of Plant Science, Seoul National University

ABSTRACT

Plants possess hundreds of intracellular immune receptors encoding nucleotide-binding domain and leucine-rich repeat (NLR) proteins that can recognize pathogen effectors. Activated NLRs confer disease resistance that is often accompanied by localized cell death termed by hypersensitive response. NLR proteins typically consist of three major domains, an N-

terminal TOLL/interleukin-1 receptor (TIR) or coiled-coil (CC) domain, a central nucleotide binding (NB-ARC) domain, and a C-terminal leucine-rich repeat (LRR) domain. The CC domain is known to function as a signal inducer and remains in an auto-inhibited state through intramolecular interaction with NB-ARC and LRR domains in absence of pathogen infection. In this study, cell death induced by genome-wide autoactive pepper NLRs and their N-terminal domain was analyzed by transient overexpression in *Nicotiana benthamiana*. The screening assay revealed that CC domain of group 10 (G10)-NLRs specifically trigger HR-like cell death. Moreover, G10-CC domain from other Solanaceae plants (tomato and tobacco) induced cell death. The G10-NLR or G10-CC domain-mediated cell death appears to mimic the HR cell death triggered by resistance protein and effector as demonstrated by the requirement of molecular chaperone complex for NLR immune signaling and upregulation of HR- and defense-related genes. VIGS-based screen designed to identify G10-NLR signaling components revealed that cell death induced by G10-NLR and G10-CC domain occurred in a SA/JA-independent manner. In addition, deletion and mutation analyses showed that the primary α-helix in G10-CC domains contribute to cell death signaling rather than to the proper targeting of the protein to the plasma membrane. To understand the molecular basis of G10-NLR-mediated ell

death, I identified S-adenosyl homocysteine hydrolase (SAHH) as a candidate of interacting protein with G10-CC domain using pull-down experiment coupled with LC-MS/MS analysis. Cell death induced by G10-NLR and G10-CC domain was compromised by co-expression with SAHH, suggesting that SAHH may function as a negative regulator of G10-NLRs. In addition, the SAHH-silenced plants exhibited constitutive H_2O_2 accumulation in absence of pathogen, implying that SAHH is a negative regulator of reactive oxygen species production. How G10-NLRs trigger cell death response remains unclear, but this study gives a clue to understand the molecular mechanisms underlying HR cell death induced by activated NLRs and the distinct role of G10-NLRs in plant immune responses.

Keywords: Pepper NLR, Autoactive NLR, Cell death, Coiled-coil domain, SAHH, Reactive oxygen species

Student number: 2013-30326

CONTENTS

LIST OF TABLES

LIST OF FIGURES

LIST OF ABBREVIATION

NLR	Nucleotide-binding domain and leucine-rich repeat
TIR	Toll/interleukin-1 receptor domain
CC	Coiled-coil
HR	Hypersensitive response
ROS	Reactive oxygen species
SA	Salicylic acid
SAH	S-adenosyl homocysteine
SAM	S-adenosylmethionine
SAHH	S-adenosyl homocysteine hydrolase

LITERATURE REVIEW

Plant immune system

Plants lack an adaptive immune system or specialized immune cells. Instead, in order to effectively protect themselves against pathogen, plants have established multi-layered defense mechanisms through the co-evolution with adapted pathogens (Schulze-Lefert, 2004). These include constitutive (preformed) defenses and induced defenses.

Constitutive defenses are usually non-specific and effective against a broad range of pathogens, and include not only physical barriers such as the thick cuticle layer, wax layer and cell wall but also antimicrobial compounds called phytoanticipins (van Hulten et al., 2006). Induced defense responses begin when plants perceive warning signal molecules derived from pathogens, leading to both accumulation of antimicrobial compounds called as phytoalexins and initiation of various defense responses. These defense reactions often culminate in a form of localized cell death termed the hypersensitive response (HR).

There are two layers of surveillance system to induce defense response by specifically detecting invasion signals. First, plasma membrane-localized receptors can perceive 'non-self' by detection of conserved pathogen structures called pathogen-associated molecular patterns (PAMPs) or 'damaged-signal' (damage-associated molecular patterns (DAMPs) defined as endogenous molecules released by not only cellular injury in plant-microbe interaction but also damages by herbivory or wounding) (Raaymakers and Van den Ackerveken, 2016). These patterns are recognized via pattern-recognition receptors (PRRs) that activate pattern-triggered immunity (PTI) (Zipfel, 2009). Reactive oxygen species (ROS) burst and callose deposition at the infection site are general defense mechanism in response to pathogen invasion in PTI. To dampen this defense responses, successful pathogens secrete a number of effector proteins into host cells (Dodds and Rathjen, 2010). In turn, plants induce a second rise in the defense level, effector-triggered immunity (ETI), via recognition of effectors by intracellular immune receptors called resistance (R) proteins, which mostly belong to the nucleotide-binding domain, leucine-rich repeat (NLR) family (Meyers et al., 1999). ETI is often followed by localized cell death that restrict the spread of pathogens at the infection site (Jones and Dangl, 2006). Activation of PTI and ETI triggers downstream defense signaling such as generation of ROS and

activation of mitogen-activated protein kinases (MAPKs) cascade, hormone synthesis and transcriptional reprogramming of defense-related genes (Jones and Dangl, 2006). The coordination of these defense responses is of importance for successful defense against pathogens.

Nucleotide-binding domain and leucine-rich repeat (NLR) genes in plant immunity

The NLR genes form a large gene family in the plant kingdom and usually possess a central NB-ARC domain (Nucleotide-Binding adaptor shared by Apaf-1, Resistance proteins, and CED-4), a C-terminal LRR (Leucine-Rich Repeat) domain, and a variable N-terminal domain. Plant NLRs are divided into two groups, depending on their N-terminal domain, CNL (CC-NB-LRR) with a coiled-coil (CC) domain and TNL (TIR-NB-LRR) with a Toll/interleukin-1 receptor domain (TIR) (Meyers et al., 2003). TIR domain has homology with the *Drosophila* toll and human interleukin-1 receptor. Although CC domains lack a conserved structure, canonical CC domains contain a 'EDVID' motif (Rairdan et al., 2008). The non-canonical CC domains without a EDVID motif, is referred to as CC_R, because CC_R domain is similar to *Arabidopsis* RESISTANCE TO POWDERY MILDEW

8 (RPW8) which has been proposed to be implicated in broad spectrum resistance to powdery mildew (Xiao et al., 2001; Collier et al., 2011).

Plant NLR proteins are activated either by direct binding to pathogen effectors, or by indirect detection of effector-induced modification in the target proteins of effectors (Mackey et al., 2002). Previously, both domain swap analysis and biochemical study of NLR proteins demonstrated that LRR domain plays an essential role in the recognition of pathogen-derived effectors (Ellis et al., 1999; Jia et al., 2000; Shen et al., 2003; Rairdan and Moffett, 2006; Rentel et al., 2008; Tomita et al., 2011). Upon recognition of effector protein(s), the central NB-ARC domain induces a conformational change to activate NLR protein (Tameling et al., 2006). Subsequently, the activated NLRs may expose the N-terminal domain to trigger downstream signaling (Qi et al., 2012).

There are several lines of evidence that support the signaling role of N-terminal domain. Mutation of the 'EDVID' motif in the CC domain of the barley resistance gene *MLA10* compromises MLA10-mediated cell death (Bai et al., 2012). In addition, overexpression of the CC or the TIR domain of several NLRs causes cell death in absence of a cognate effector (Weaver et al., 2006; Krasileva et al., 2010; Bernoux et al., 2011; Collier et al., 2011; Maekawa et al., 2011; Wang et al., 2015; Cesari et al., 2016; Hamel et al.,

2016). Recently, it has been proposed that the N-terminal domains could also play a role for effector recognition. For example, CC domain of *Arabidopsis* RPM1 detects RIPK-dependent phosphorylation of RIN4 (RPM1-interacting protein 4) by AvrB and AvrRPM1 (Mackey et al., 2002). Moreover, CC domain of *Arabidopsis* RPS2 (Resistance to *Pseudomonas syringae* 2) is capable to sense the fragment of RIN4 cleaved by AvrRpt2 (Mackey et al., 2003). It is highly plausible that N-terminal domains of NLRs might be responsible for monitoring effector-induced posttranslational modification of their target protein.

As mentioned above, NLR proteins activate the ETI signaling upon recognition of pathogen attack. For the last several decades, many studies have focused on understanding the molecular basis of ETI. Nevertheless, the molecular mechanism of ETI in plant-microbe interaction is still largely unknown.

Hypersensitive response in disease resistance

Pathogen recognition via NLRs leads to resistance and the inhibition of pathogen proliferation. Plant resistance response is often, but not always, accompanied by rapid cell death of the infected cell and surrounding cells. This response is called HR which is a form of programmed cell death. The

observation of HR was first reported in the wheat-brown rust pathosystem in 1902. This phenomenon was termed as ‘hypersensitiveness’ by Stakman (Ward, 1902; Stakman, 1915). Morphologically, HR presents specific features of programmed cell death which is characterized by cell shrinking, chromatin condensation, DNA fragmentation, mitochondrial swelling, vacuolization and chloroplast disruption. A series of these cellular processes in HR-cell death in plant is known to be similar to those of apoptosis in animal (Reape et al., 2008; Coll et al., 2011).

Although HR is suicide mechanism upon plant-microbe interaction, plants have evolved it as common and effective defense mechanism to let neighbor cells be aware of the pathogen invasion for the benefit of the whole plant. By rapidly sacrificing infected cells, the plant restricts the supply of nutrients required for survival and growth of biotrophic or hemibiotroph pathogen in host cells.

However, it is important to note that whether HR cell death is required for resistance to pathogens remains unclear. Cell death often seems not to be required for successful activation of resistance although HR cell death may be genetically controlled by the host. For example, disease resistance can occur in the absence of macroscopic HR-like cell death in nature, which is called an extreme resistance (Longstaff et al., 1993; Sekine et al., 2008).

Moreover, mutation of the *Arabidopsis ndr1* (non-race-specific disease resistance1) rendered the plant susceptible to *Pseudomonas* spp. and *Peronospora* spp., although HR-like cell death was still induced (Century et al., 1995). Conversely, *Arabidopsis dnd2 (defense, no death 2*) mutants did not exhibit HR but gained broad spectrum resistance against *Pseudomonas* in association with constitutively elevated levels of both endogenous salicylic acid (SA) contents and *PR1* gene expression (Jurkowski et al., 2004).

However, it has been getting clear that cell death induced by activated NLR is apparently connected with resistance to pathogens. Mutations of CC domain in MLA10 lead to an impaired cell death activity resulting in the loss of disease resistance to *Blumeria graminis* f. sp. *Hordei* (Maekawa et al., 2011; Bai et al., 2012). In addition, most of HR cell deaths are accompanied by transcriptional activation of various defense-related genes, accumulation of SA and ROS generation (Mur et al., 1997; Tornero et al., 1997). These responses are typical ETI features that enable to distinguish between HR and a necrotic cell death. Furthermore, several effectors delivered from bacteria and oomycete are capable of suppressing HR in plants (Abramovitch et al., 2003; Bos et al., 2009; Guo et al., 2009). Therefore, HR cell death generally has been regarded as a consequence of the rise in a series of defense responses rather than physical restriction of pathogen spread-out at the infection site.

Autoactivation of NLRs

When exposed to biotic stresses, plants invest their energy in a variety of stress-related cellular and biochemical processes rather than into their growth and development. This reduction of growth and reproduction is called a 'fitness cost'. Most studies have shown that the tradeoff for the fitness costs appears to be regulated by manipulating the SA and the JA signaling pathway, which play an important role in defense response (Heil and Baldwin, 2002).

Since plants utilize NLR proteins to recognize specific pathogen effectors for activation of immunity in response to biotic stress, activated NLR proteins trigger strong immune responses such as HR. Therefore, it is necessary for plants to develop elaborate mechanisms which control expression level of NLR genes and protein stability. NLRs must be strictly regulated not only to avoid uncontrolled immune activation but also to prevent growth inhibition (Karasov et al., 2017).

NLR proteins exist in an autoinhibited state (OFF state) to avoid the activation of immune responses in the absence of pathogen infection. The central NB-ARC domain in a NLR protein has an important role to switch between ON/OFF states (Takken et al., 2006). In the OFF state when bound to adenosine diphosphate (ADP), the nucleotide-binding pocket in the NB-ARC domain has a closed form. After pathogen recognition, the nucleotide-

binding pocket is partially opened, allowing to replace the ADP with adenosine triphosphate (ATP). The ATP-bound form is able to return to the ADP bound conformation via intrinsic ATPase activity in the absence of a pathogen effector. Mutations of the NB-ARC domain disrupting the inhibited state causes autoactivation of several NLRs, resulting in constitutive immune responses without the interaction between hosts and microbe (Bendahmane, 2003; Howles et al., 2005; Van Ooijen et al., 2008; Gao et al., 2011; Williams et al., 2011).

Inactive state of NLR protein is also tightly maintained by intramolecular interactions with other subdomains of NLRs (Heidrich et al., 2013; Cesari et al., 2014; Sukarta et al., 2016). Activity of the CC domain or NB-ARC is usually suppressed by intramolecular interaction with LRR domain (Moffett et al., 2002; Leister et al., 2005; Slootweg et al., 2013; Chen et al., 2016; Kim et al., 2018). It has been shown that deletion of LRR domain of several NLRs causes autoactivation (Rairdan et al., 2008; Qi et al., 2012; Kim et al., 2018). In addition, domain-swap between closely related NLRs, such as Rx1 and Gpa2 from potato, and RPS5 (Resistance to *Pseudomonas syringae* 5) and RPS2 from *Arabidopsis*, resulted in constitutive activation due to incompatibility between subdomains (Rairdan and Moffett, 2006; Qi et al., 2012; Slootweg et al., 2013).

This inactive state is also controlled by intermolecular interactions with other NLR proteins. Overexpression of the full length *RGA4* in rice or either *RPS4* in *Arabidopsis* trigger cell death in *N. benthamiana*. However, co-expression of their partner NLR, full-length *RGA5* or full-length *RRS1* respectively, compromises an autoimmune response through formation of the heterodimerized complex (Zhang et al., 2004; Day et al., 2005; Cesari et al., 2014). In case of RPS4, heterodimerization between TIR domains of RPS4 and RRS1 enables to retain the inactive state of RPS4 (Williams et al., 2014).

Recently, it was revealed that hybrid necrosis is caused by autoimmune responses due to the cooperation between natural genetic variants of NLRs. *Arabidopsis DM1* and *DM2d* are two TNLs from two different *Arabidopsis* ecotypes, Uk-3 and Uk-1, and the interaction between these proteins results in autoactive immune responses leading to necrosis and hybrid incompatibility during a cross between two ecotypes (Chae et al., 2014; Tran et al., 2017)

Cell death induced by the Autoactive N-terminal domain of NLRs

The N-terminal domain of NLRs is proposed to serve as signal initiator based on several experimental evidences. Overexpression of the N-terminal domain of different NLRs has been shown to induce cell death in absence of

a corresponding effector protein. Frost et al., 2004 demonstrated that TIR domain and extra 39 amino acids (aa) of flax (*Linum usitatissimum*) L10 resistance protein trigger effector-independent cell death in tobacco. Similarly, the fragments of TIR domain in polymorphic *L* loci, L6 and L7, grape RPV1, *Arabidopsis* RPS4, RPP1 and SNC1 were reported to induce the effector-independent cell death (Weaver et al., 2006; Krasileva et al., 2010; Bernoux et al., 2011; Williams et al., 2016; Zhang et al., 2017). These results indicate that TIR domain itself triggers cell death in absence of pathogen recognition. Taken together, the TIR domain appears to play an important role as an inducer of death signal.

TIR domain–triggered cell death depends on defense-related signal pathway. For example, cell death induced by the RPS4-TIR domain was notably impaired in plants silenced for *EDS1*, *HSP90* and *SGT1* genes which are known to function in NLR-mediated resistance (Swiderski et al., 2009). Stunted plant phenotype was also observed in L10-TIR domain overexpressing plants correlated with a high level of *PR1* transcripts and constitutive expression of defense genes (Frost et al., 2004).

Similar to the TIR domain, the transient expression of CC_R domain of *Arabidopsis* ADR1 and tobacco NRG1 and the typical CC domains of barley MLA10, wheat Sr33 and potato Rp1 trigger cell death in *N. benthamiana*

(Collier et al., 2011; Maekawa et al., 2011; Wang et al., 2015; Cesari et al., 2016). Recently, CC domains derived from several I2-like NLRs in Solanaceae were also shown to induce cell death (Hamel et al., 2016).

Cell death induced by the autoactive N-terminal domain of NLRs often associates with self-association activity (Bernoux et al., 2011; Maekawa et al., 2011; Casey et al., 2016). The crystal structure of the TIR domain of L6 revealed an interface for TIR homodimerization (Bernoux et al., 2011). Analysis of the crystal structure combined with site-directed mutagenesis in the TIR-TIR interface revealed that self-association is necessary to trigger cell death. Similarly, the CC domain of MLA10 is also able to form homodimer and mutations of residues at the dimer interface between CC domains disrupted the activation of cell death (Maekawa et al., 2011). Moreover, TIR domain of RPP1 and CC domain of maize RP1-D21 and RP1-D trigger cell death when fused to a wild type GFP (green fluorescent protein) tag which can form dimer *in planta,* implying that auto-association through the eGFP tag mimics the activated state of the N-terminal domain (Krasileva et al., 2010; Wang et al., 2015).

INTRODUCTION

As the first step of the elaborated and multi-layered defense mechanism activated upon pathogen attack, plants have developed a surveillance system to recognize the presence of 'non-self' molecules or endogenous 'danger signals', which are released as by-products from damaged cells (Cook et al., 2015). The second mode is triggered by recognition of pathogen-derived effector proteins which are translocated into host cells from pathogen to modulate host defense system in a variety of ways (Jones and Dangl, 2006).

One of the monitoring system is based on a resistant (R) protein including nucleotide-binding and leucine-rich repeat (NLR) composed of three major domains - a variable N-terminal domain, a central nucleotide binding (NB-ARC) domain and a C-terminal leucine-rich repeat (LRR) domain. NLR genes belong to one of the largest gene families *in planta* and can be divided into two major groups based on the N-terminal domain (Jones and Dangl, 2006; Meyers et al., 2003). One group contains the Toll/interleukin-1 receptor (TIR) domain at the N-terminus, referred to as TIR type-NLR (TNL), the other possesses N-terminal domain with a coiled-coil (CC) structure, referred

to as CNL type-NLR (CNL) (Jones and Dangl, 2006). In CNL type NLRs, NLRs with the N-terminal CC domains resembling *Arabidopsis* resistance protein RPW8 were considered as a distinct subclass RPW8-type CNL (CNL-R) based on their function in the downstream signaling (Peart et al., 2005; Bonardi et al., 2011; Collier et al., 2011).

NLR proteins can sense the presence of effector proteins by binding them directly or indirectly as well as by perceiving posttranslational modification of the host target proteins. Following recognition of the effectors, NLR proteins undergo a conformational change by replacing ADP with ATP at the central NB-ARC domain, resulting in activation of NLR proteins. Activated NLRs enables to initiate a variety of intracellular biochemical and physiological changes such as upregulation of defense-related genes and generation of various reactive oxygen species (ROS) (Mestre and Baulcombe, 2006; Bernoux et al., 2011; Maekawa et al., 2011). Consequently, these features culminate in a hypersensitive response (HR) at the infection site to arrest pathogen growth.

NLRs require well conserved downstream signaling components, including the nucleocytoplasmic lipase-like protein Enhanced disease susceptibility 1 (EDS1) or the plasma membrane-localized protein Non-race specific disease resistance 1 (NDR1) for TNL and CNL classes, respectively

(Jones and Dangl, 2006). These two branches of NLR signaling require conserved chaperone complex containing *SGT1* (Suppressor of the G2 allele of SKP1), *HSP90* (Heat shock protein 90) and *Rar1* (Required for MLA12 resistance 1), which play a role as a hub to maintain homeostasis of NLR proteins (Shirasu, 2009). NLRs have also shown a requirement for the defense hormone, salicylic acid (SA) for disease resistance and induction of systemic acquired resistance (SAR).

To activate NLR-mediated immunity, N-terminal domain of NLR proteins plays multiple regulatory roles. In case of several NLRs, the N-terminal domain physically interacts with host target proteins which are manipulated by effector proteins (Mucyn et al., 2006; Ade et al., 2007; Burch-Smith et al., 2007; Sacco et al., 2007). *Arabidopsis* RIN4 is phosphorylated or cleaved by AvrRpm1 or AvrRpt2 from different pathovars of *Pseudomonas syringae,* which are recognized respectively by RPM1 or RPS2 through their N-terminal domains (Mackey et al., 2002; Day et al., 2005). In addition, interaction between homotypic N-terminal domains contribute to form high-order complexes of NLRs upon activation (Mestre and Baulcombe, 2006; Bernoux et al., 2011; Meakawa et al., 2011). For example, mutation in CC domain of barley MLA10 impairs dimerization and consequently affects full-length MLA10-mediated cell death (Maekawa et al., 2011). Moreover,

N-terminal domain of NLRs is also involved in transducing cell death signal. Overexpression of the N-terminal region only of several NLRs is sufficient to trigger cell death signaling (Peart et al., 2005; Bernoux et al., 2011; Bonardi et al., 2011; Collier et al., 2011, Maekawa et al., 2011; Casey et al., 2016; Hamel et al., 2016). However, it still remains unclear how the N-terminal domain of NLRs transduces the defense signal and what components are required to trigger cell death.

The Solanaceae family is a large plant family that consists of about 2,300 species encompassing economically important crops such as potato, tomato and pepper (Chiarini and Bernardello, 2006). Comparative analysis of NLR genes across Solanaceae genomes revealed that the NLR gene family can be classified into 14 subgroups, including one TIR-NLR (TNL) subgroup and 13 CNL subgroups (Seo et al., 2016). Among them, CNL-Group 10 (G10) is composed of 34 genes including a known pepper resistance gene, *Pvr4,* which confers resistance to Potyviruses such as *Potato virus* Y (PVY) and *Pepper mottle virus* (PepMoV) through the recognition of a viral effector, NIb (Kim et al., 2015; Kim et al., 2017). Recently, structural domain analysis revealed that the CC domain of Pvr4 is sufficient to activate cell death in absence of NIb (Kim et al., 2018).

In a genome-wide screening for autoactivity of pepper NLRs and their N-terminal domains, we found that CC domains of distinct G10-NLRs specifically induce cell death at a high rate. To better understand the signaling pathway associated with this cell death response, I performed pull down assay coupled with LC-MS/MS and identified S-adenosyl homocysteine hydrolase (SAHH) as a candidate for G10-CC domain-interacting protein.

SAHH is one of the most conserved enzymes in all organisms and catalyzes the hydrolysis of S-adenosyl homocysteine (SAH) to adenosine and L-homocysteine (Palmer and Abeles, 1979). Since homocysteine is used for a recycling reaction to produce S-adenosylmethionine (SAM) which functions as a primary methyl donor, SAHH plays a pivotal role as a key enzyme to activate methylation processes on proteins, nucleic acids, and polysaccharides. SAM also serves both as a precursor for the production of ethylene and as a substrate in the biosynthesis of polyamines (Smadar harpaz-Saad, 2012). Indeed, *Arabidopsis SAHH1* mutant shows embryo-lethal phenotype, therefore SAHH is necessary in vital processes in the cell (Rocha et al., 2005). It has been reported that SAHH also engages in plant defense response. Transgenic tobacco expressing antisense RNA for *SAHH* showed inhibition of viral replication and resistance against a variety of plant viruses including *Tobacco mosaic virus*, *Potato virus* X, *Cucumber mosaic virus* and

PVY (Masuta et al., 1995). The resistance may be driven by inhibition of 5' capping in viral RNA replication or given by high accumulation of cytokinins. Moreover, SAHH transcript level was highly increased in a potato cultivar susceptible to *Phytophthora infestans*, but not in a resistant cultivar (Arasimowicz-Jelonek et al., 2013). Furthermore, *SAHH*-silenced tomato showed significantly increased SA contents in both infected and uninfected plants. *SAHH*-silenced tomato also exhibited constitutively activated immune responses accompanied by up-regulated defense-related genes, callose deposition and ROS accumulation (Li et al., 2015). Although all of these evidences imply that SAHH negatively regulates defense responses in plants, it is still unknown how plants regulate SAHH activity in response to pathogens.

In this study, *SAHH*-silenced *N. benthamiana* plant exhibits cell death speckles and accumulation of ROS. In addition, co-expression of SAHH reduced cell death induced by pepper G10-NLR and G10-CC. Although the evidence for direct interaction of G10-CC domain with a SAHH protein is not presented here, these results imply that G10-CCs induce cell death by having a negative effect on SAHH activity.

CHAPTER III. MATERIALS AND METHODS

Plant materials and growth condition

N. benthamiana plants were grown under a 16-hr/8hr photoperiod at 25°C in horticultural bed soil (Baroker, Seoul Bio Co., Ltd., Seoul, Korea). Four-week old plants were used for transient overexpression. For Virus-Induced Gene Silencing (VIGS) experiments, foliage leaves of 2-week old plants were inoculated with *Agrobacterium*.

Plasmid construction

Pepper NLRs were amplified from genomic DNA of *Capsicum annuum* L. cv Criollo de Morelos 334 (CM334) based on pepper reference annotation v.1.55. N-terminal domain of NLRs were defined from methionine to just before the first motif (p-loop) in NB-ARC domain. cDNAs from the *N. benthamiana* expressing G10-NLRs or CC domains, or silenced plants were used as templates for PCR amplification using PrimeSTAR pfu polymerase (TaKaRa, Shiga, Japan).

For transient overexpression in *N. benthamiana*, PCR fragments were cloned in the pCAMBIA2300-LIC vector containing cauliflower mosaic virus 35S promoter and nopaline synthase terminator by ligation-independent cloning (LIC) method (Aslanidis and de Jong, 1990; Oh et al., 2010). The *ccdB* (lethal) gene was inserted into pCAMBIA2300 vector to facilitate LIC system. Gene specific primers carrying the LIC adaptor sequence were used to amplify DNA fragment. PCR products purified by magnetic bead type PCR cleanup kit (Biofact, Daejeon, Korea) and *PstI*-digested pCAMBIA2300-LIC or pCAMBIA2300-3xFLAG-LIC vector were treated with T4 polymerase to create single-stranded overhangs on vector and DNA insert. Treated vector and DNA insert were mixed to annealed to each other and the mixture was transformed into *Escherichia coli* DH5α strain. The N-terminal substitutional mutations were generated using primers carrying the mutations. PCR products were cloned into pCAMBIA2300-LIC or pCAMBIA2300-3xFLAG-LIC vector. All constructs used in this study were sequenced to confirm their identity.

Agrobacterium*-mediated transient overexpression in *N. benthamiana

Agrobacterium tumefaciens GV3101 strains carrying the various constructs are prepared for transient overexpression in *N. benthamiana*.

Agrobacteria were grown overnight at 28°C in LB media supplemented with kanamycin (50 μg/ml) and rifampicin (50 μg/ml). Agrobacteria cultures were precipitated and resuspended in infiltration buffer (10 mM MES (pH 5.6) and 10 mM $MgCl_2$ with 150 μM acetosyringone) at optical density at 600 nm ($O.D_{600}$) = 0.3 for CC domains or 0.8 for *Pvr4* or 0.4 for *NIb*. Agrobacterial suspensions were infiltrated on the abaxial leaves of 4-week-old *N. benthamiana* plants with a needleless syringe. Macroscopic cell death phenotypes were scored at 5-day post infiltration.

Measurement of electrolyte leakage

Three leaf discs were collected with a No. 7 corer from three independent plants infiltrated 24 hr earlier. Leaf discs were washed briefly in water, and moisture on leaf discs was gently removed with a paper towel. Washed leaf discs were submerged in 5 mL of distilled water with 0.001 % silwet L-77 at room temperature (three replicates per sample). Twenty-four hours later, electrolyte leakage was measured with an Orion Model 215 (Thermo scientific, Waltham, MA, USA).

Virus-induced gene silencing (VIGS)

The target gene region was amplified from *N. benthamiana* cDNA and cloned into the pTRV2-LIC vector using a LIC method (Dong et al., 2007). VIGS constructs were transformed into *Agrobacterium tumefaciens* strain GV3101 by the freeze-thaw method. Agrobacteria carrying pTRV1 and pTRV2 containing a specific gene fragment were grown overnight in Luria-Bertani (LB) broth with 50 μg/ml kanamycin and 50 μg/ml rifampicin at 28°C with vigorous shaking. Agrobacteria cultures were precipitated and resuspended in infiltration buffer (10 mM MES (pH 5.6) and 10 mM $MgCl_2$ with 150 μM acetosyringone). A suspension of pTRV1 and pTRV2 carrying a target gene fragment were mixed at final optical density at 600 nm ($O.D_{600}$) = 0.15 respectively. Two leaves of 3-week old *N. benthamiana* seedlings were infiltrated with Agro-suspension culture. Two weeks later, top leaf of silenced plants was collected to confirm the silencing of the target gene.

Quantitative RT-PCR

Total RNA was extracted using TRIzol reagent (MRC, OH, USA) and complementary DNA was synthesized using Superscript III (Invitrogen, CA, USA). Gene-specific primers were used in quantitative RT-PCR at 95 ℃ for 5 min, followed by 40 cycles with denaturation at 95 ℃ for 15s, 55 ℃ for 1 min. Power SYBR green PCR master mix (Applied biosystems, Foster city,

CA). Nucleotide sequences of all primers used in this study are listed in Table 1. Level of gene transcripts was normalized to that of elongation factor gene, *NbEF1-α*.

Confocal laser scanning microscopy

Plant tissues expressing eGFP-tagged proteins were examined with a Leica confocal microscope SP8X (Leica Microsystem, Germany). eGFP was imaged using 488 nm excitation and its emission signal was detected from 500 nm to 530 nm. Simultaneous excitation of eGFP and plasma membrane marker dye, FM4-64 (Invitrogen, CA, USA) was performed using the 488 nm excitation and emission signal was collected 500-530 nm and 600-650nm for eGFP and FM4-64, respectively.

Immunoprecipitation

Leaves were ground in liquid nitrogen and extraction buffer (50 mM Tris-HCl (pH 7.5), 100 mM NaCl, 1 mM EDTA, 1% (v/v) IGEPAL CA-630, 10 % glycerol, 5 mM DTT, 1 mM NaF, 1mM PMSF, 1x protein phosphatase inhibitor cocktail (P9599, SIGMA, Darmstadt, Germany) was added at 2 mL/g tissue powder. Samples were incubated at 4℃for 1 h with gentle rolling to solubilize the plasma membrane and then clarified by 20 min centrifugation

at 12,000 rpm. Supernatants were diluted to 3 mg/ml protein using extraction buffer and incubated with 100 μL of anti-FLAG M2 magnetic beads (M8823, SIGMA, Darmstadt, Germany). Following incubation for 1 hr, magnetic beads were washed five times with extraction buffer. Elution buffer containing 500 ng/μL FLAG peptide were added to beads and incubated with gently shaking for 1 hr at 4℃. LC-MS/MS analysis was performed using Orbitrap mass spectrometers (Thermo Scientific, Massachusetts, U.S.A).

DAB staining

Accumulation of hydrogen peroxide (H_2O_2) was detected with 3,3'-Diaminobenzidine (DAB) staining. *N. benthamiana* leaves were detached and incubated in DAB-HCl solution (1 mg/ml, pH 3.8) overnight at 25°C in the dark. After staining, the leaves were soaked in 95% ethanol to remove chlorophyll.

Quantification and statistical analysis

Error bars in all of the figures represent standard deviations of mean. Number of replicates is reported in the figure legends. Statistical comparison among different samples is carried out by one-way ANOVA with Tukey's

HSD (honest significant difference) test. Samples with statistically significant differences ($p < 0.05$) are marked with different letters (a, b, c etc.).

Table 1. List of primers used in this study

Primer name	Forward(5'→3')	Reverse(5'→3')	Ref.
For VIGS			
NbHSP90	AGAAGCACTCTGAGTTCATCAG	ATCAACCATGTAAAGAACCTC	(Liu et al., 2004)
NbSGT1	ATATACGAGAGCGTCTGCTG	CAGTCCCATTAGATTCCACA	(Anand et al., 2012)
NbICS2	ATCTTAAACTCATCATCTTCAGCC	GCAGGCTTCGCCGGCATTCATTGG	(Zhu et al., 2014)
NbNPR1	GCTGTGGCATTCCTGGTT	GTGAGCCTCTTGGCGATT	(Zhu et al., 2014)
NbCOI1	AGAGGTTGCTATAAGCTTAGA	TCAGTGGCAACAACTCGTCT	(Yoon et al., 2009)
NbWIPK	CGCCAGCAGTTAGCAAATG	GTCGAAGGAGAATGGAACG	(Li et al., 2015)
NbSIPK	GCTGCAATTGATCTTGTCGAG	GGCATGCTGTTCAAAGTCGA	(Li et al., 2015)
NbNDR1	CATGTCAAACTATGGATCCAA	GTCATGACCTTGGTAAAAGCCAGGTA	
NbEDS1	GAGAATCCAGATGCTGTTCTGCAG	GAACCACATCCTGCATCTCTAAGC	
GFP	ACGTAAACGGCCACAAGTTC	GGGGTGTTCTGCTGGTAGTG	

For qRT-PCR			
NbHSP90	CAACCCGGAG AATGCTATTA	TCCATCTTGCTACCTT CAGC	
NbSGT1	TTTGTGGAATCTAAT GGGAC	CAAACAAAACAAAC GTCAC	
NbICS2	TTGATGAGCTTGAAG GAAGT	GGGACATGAGTACTC GCG	
NbNPR1	TAAGGTGGAATTAAA GGAAATA	TAGGTGAAGGCCTAA TTTTT	
NbHIN1	GCCATGCCGGAATCC AATTT	TTGCAGAGGCAGCCA AAGAGA	(Moon et al., 2016)
NbPR1	AATAGGGTAGCGGCC TTTGC	CGGCGGCTAGGTTTT CG	(Moon et al., 2016)
NbCYP71D20	CCGCACCATGTCCTT AGAG	CTTGCCCCTTGAGTA CTTGC	(Heese et al., 2007)
NbWRKY8	AACAATGGTGCCAAT AATGC	TGCATATCCTGAGAA ACCATT	(Heese et al., 2007)
NbEF1-a	GTATGCCTGGGTGCT TGAC	ACAGGGACAGTTCCA ATACCA	(Heese et al., 2007)

CHAPTER IV. RESULTS

The autoactive N-terminal domain of pepper G10-NLRs causes cell death in *N. benthamiana*

Previously, 755 pepper NLR genes were predicted and divided into 15 subclasses based on amino acid sequences of their NB-ARC domain by phylogenetic analysis and clustering program (Seo et al., 2016). Among 755 NLRs, genomic fragments of 468 genes which contain an intact form of domain structures were subjected to amplification and 415 were successfully inserted into binary vector pCAMBIA2300.

It was reported that overexpression of several NLR-type functional resistance (R) genes induce cell death in absence of the cognate effector, the so called autoactivity (Axtell et al., 2003; Cesari et al., 2014; Heidrich et al., 2013). In addition, overexpression of only N-terminal domain of several R proteins induces cell death, suggesting that the N-terminal domain of NLR proteins plays a role in defense signaling (Collier et al., 2011; Maekawa et al., 2011; Wang et al., 2015; Cesari et al., 2016).

To screen out autoactive pepper NLRs to induce cell death, 415 full-length NLRs were transiently overexpressed in *N. benthamiana*. Only 16 full-length NLRs induced cell death (Table 2). These genes belong to diverse groups such as group TNL (GT) group, CNL-G1, G5, G9, G10, G11 and CNL-none-grouping (NG). The group containing the largest number of autoactive NLR was GT (six genes) followed by CNL-G10 (three genes) and CNL-NG (three genes).

Next, to investigate cell death caused by their N-terminal domains (NTDs), more than 10 % of pepper NLRs assigned to each group were selected as representative NLRs based on phylogenetic tree analysis. Out of 131 tested NTDs, 21 NTDs were found to induce cell death when overexpressed in *N. benthamiana*. Interestingly, 17 out of 21 NTDs inducing cell death were included in G10. Therefore 70.8% CC domains of G10 pepper NLRs are likely trigger of cell death in *N. benthamiana* (Figure 1, Table 2). These results suggest that overexpression of the CC domains of pepper G10-NLRs specifically leads to autoactivity.

To verify that the G10-NLRs tested in this screening are transcriptionally expressed genes, transcript level of G10-NLRs was analyzed in pepper upon infection of *Phytophthora capsici* (Figure 2) (Kim et al., 2018). Although transcript level of most of G10-NLRs was sustained low (less than RPKM

value 40), two third of G10-NLR tested in this study were expressed in pepper, suggesting that G10-NLRs might be functional genes. Expression level, however, was not correlated with autoactivity of G10-NLRs and rather tends to be lower upon infection of *P. capsici* (Figure 2).

Additionally, phylogenetic tree was constructed using the amino acid sequences of G10-CC domains by maximum likelihood method. G10-CC domains divided into three subclades (Figure 3). Most of non-autoactive G10-CC domains were included in subclade I, whereas most of autoactive CC domains were grouped in subclade II or III (Figure 3). The G10-NLRs which belong to subclade I, II or III are physically clustered at chromosome 9, 1, and 10, respectively (data not shown), suggesting that G10-NLRs might undergo tandem or proximal gene duplication (Seo et al., 2016).

To see whether cell death induced by the G10-CC domains is specific in pepper or not, CC domains of G10-NLRs were identified from other Solanaceae species such as tomato, tobacco (*Nicotiana tabacum*) and *N. benthamiana*. Eight CC domains from tomato G10-NLRs and two from tobacco and two from *N. benthamiana*, were overexpressed in *N. benthamiana* in the same way as tested for the pepper G10-CCs. Interestingly, half of tested CC domains of tomato and tobacco G10-NLRs, but not those of *N. benthamiana* G10-NLRs, triggered cell death (Figure 4). These results

suggest that G10-NLRs in *N. benthamiana* may have lost cell death- inducing activity through the CC domain after speciation events. However, I could not exclude the possibility that *N. benthamiana* G10-NLRs carrying the autoactive CC domain were missed in this screening due to low quality of the annotated gene set of *N. benthamiana*. Nevertheless, the capability to induce cell death for G10-CC domains seems conserved in most of Solanaceae plants.

Table 2. Screening for cell death-inducing activity of full-length or N-terminal domain of pepper NLRs in *N. benthamiana*

Group*	No. assigned NLR	Full-length NLR**			N-terminal domain		
		No. Tested NLR	No. autoactive NLR	Autoactive NLR, %	No. tested NTD	No. autoactive NTD	Autoactive NTD, %
TNL	54	44	6	13.7	16	2	12.5
CNL-G1	75	63	1	0	10	0	0
CNL-G2	91	77	0	0	14	0	0
CNL-G3	23	20	0	0	8	0	0
CNL-G4	32	29	0	0	9	0	0
CNL-G5	10	10	1	9.1	4	0	0
CNL-G6	26	24	0	0	5	0	0
CNL-G7	18	16	0	0	7	0	0
CNL-G8	14	14	0	0	6	0	0
CNL-G9	48	46	1	2.2	9	0	0
CNL-G10	34	30	3	10	24	17	70.8
CNL-G11	7	7	1	14.3	5	1	20
CNL-G12	9	9	0	0	5	0	0
CNL-G13	1	1	0	0	1	0	0
CNL-NG	24	24	3	12.5	8	2	25
Total	466	414	16		131	21	

*Seo et al., 2016
**Choi, 2017

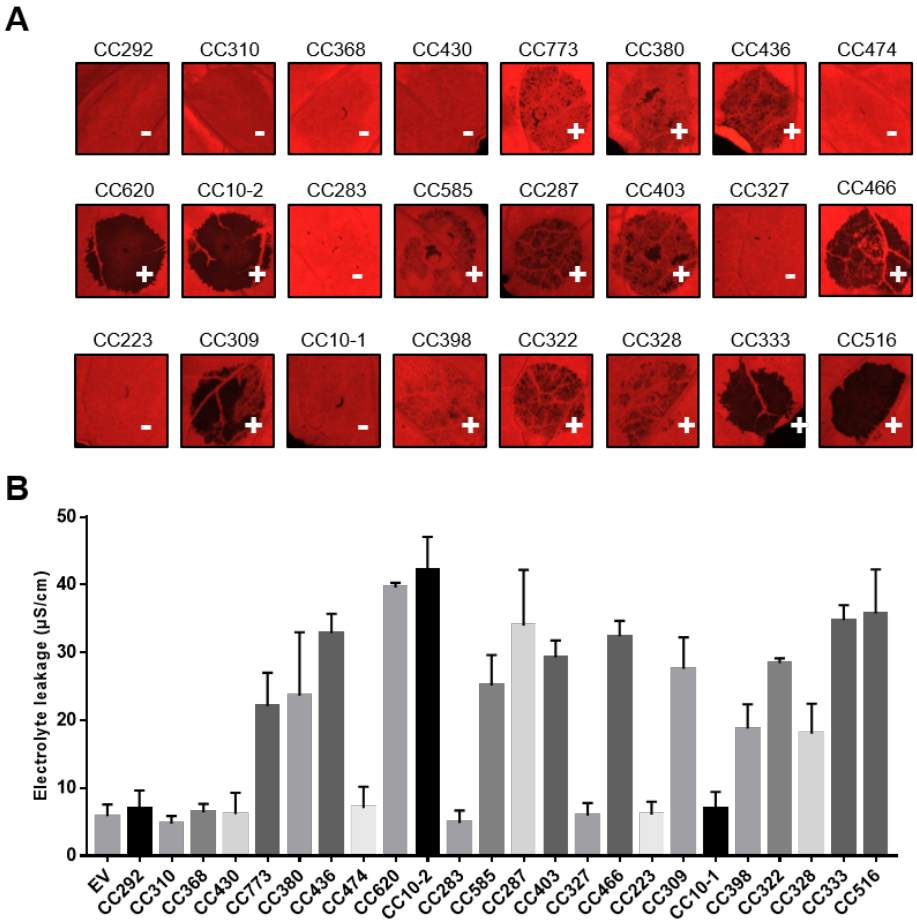

Figure 1. The CC domain of pepper G10-NLRs induce cell death when expressed in *N. benthamiana.*

(A) G10-CC domains were expressed by *Agrobacterium*-mediated transient expression method *in N. benthamiana*. Leaf discs were photographed at 3 days after infiltration. (B) Cell death activity was quantified by measuring electrolyte leakage at 48 hour post infiltration (hpi) as an indication of cell death in plants shown in (A).

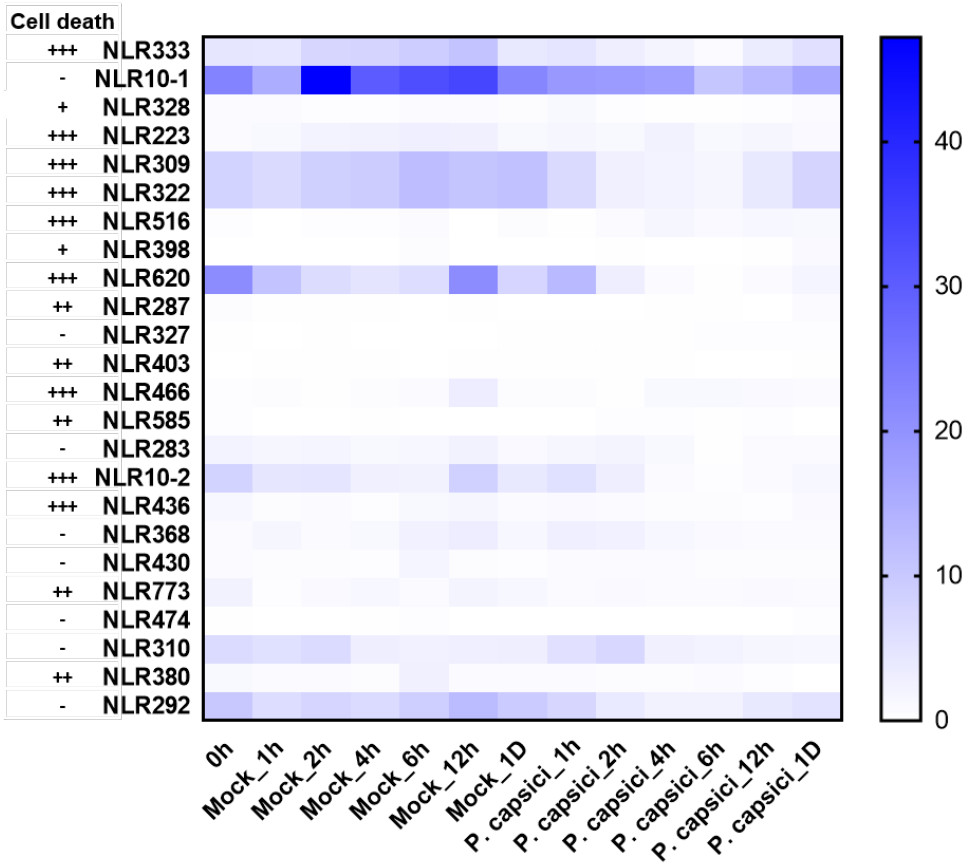

Figure 2. Transcript accumulation of the pepper G10-NLRs upon pathogen infection.

Heatmap represents the digital expression profiles of the pepper G10-NLRs over a time course of *Phytophthora capsici* infection. Color key represents reads per kilobase per million mapped reads (RPKM) values. Intensity of autoactivity of the G10-NLRs are represented at the left.

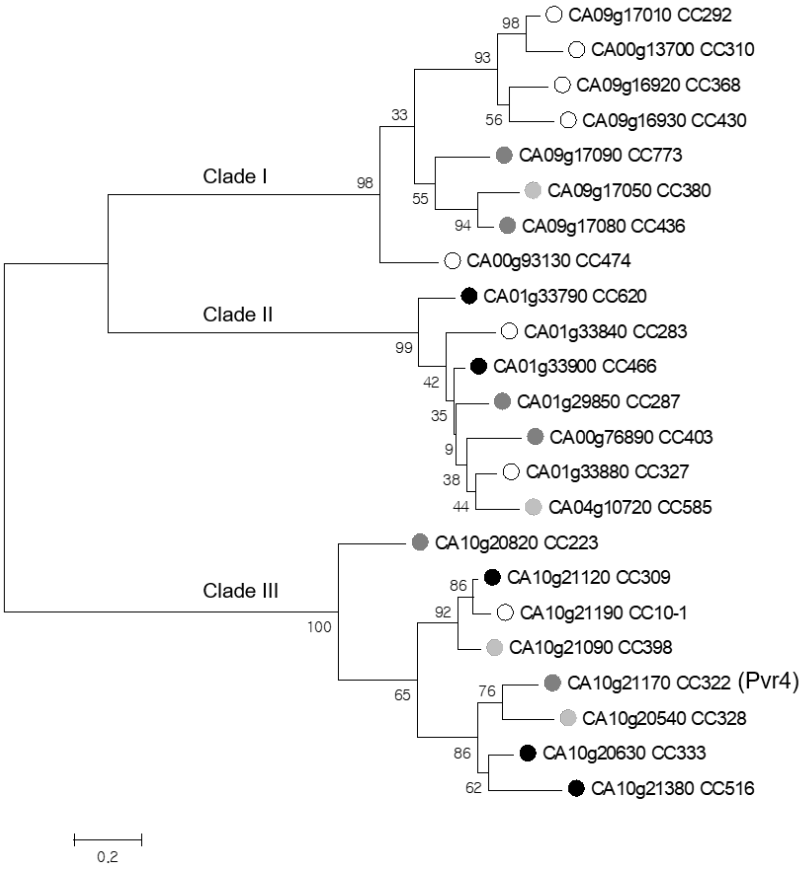

Figure 3. Phylogenetic tree of pepper G10-CC domain.
A phylogenetic tree was constructed using amino acid sequences of pepper G10-CC domains. Maximum likelihood model was used and bootstrap analysis was performed with 1000 replicates. The intensity of cell death was represented at the left side of gene ID (closed circle, strong; shaded circle, medium; open circle, no cell death).

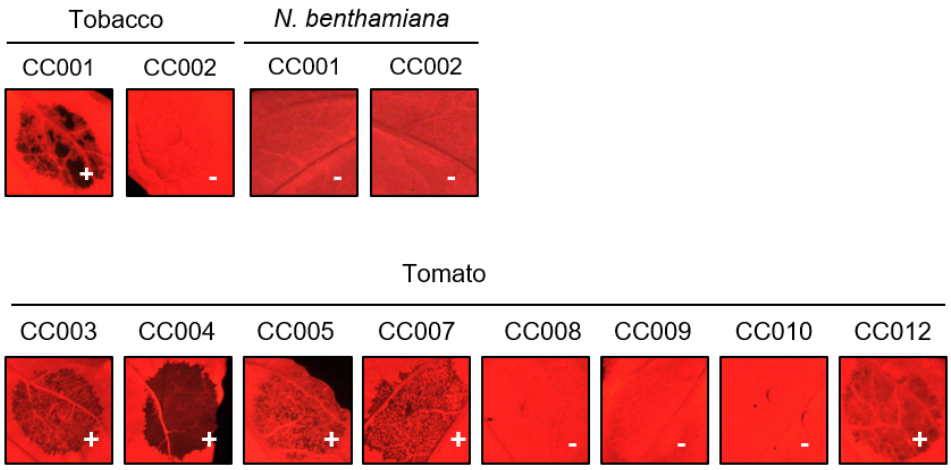

Figure 4. The CC domain of the tobacco and tomato G10-NLRs induce cell death in *N. benthamiana*.

The CC domains of NLRs in *N. tabacum* (Tobacco), *N. benthamiana* and *Solanum lycopersicum* cv. *Heinz* (Tomato) were overexpressed in *N. benthamiana* by *Agrobacterium*-mediated transient expression method. Leaf sectors were photographed at 3 days after infiltration. Induction of cell death was scored as presence (+) or absence (-).

Cell death induced by G10-NLR or G10-CC domain is associated with defense signaling pathway

Pepper G10-NLRs include a known R protein, Pvr4, which confers resistance against Potyviruses such as PVY and PepMoV by recognition of a viral effector protein NIb (Kim et al., 2017). It was recently shown that co-expression of both *Pvr4* and *NIb* triggers HR-like cell death in an *HSP90-,* and *SGT-* dependent manner (Kim et al., 2018). *HSP90* and *SGT1* are components of molecular chaperon complex and required for NLR-mediated disease resistance (Austin et al., 2002; Kadota et al., 2010).

To characterize types of cell death induced by autoactive G10-CC, I first tested whether the G10-CC domain-mediated cell death is involved in defense responses or not. *HSP90* and *SGT1* were silenced in *N. benthamiana* using virus-induced gene silencing (VIGS), followed by the transient overexpression of one of autoactive G10-CC, CC309. Silencing efficiency was confirmed by qRT-PCR using gene-specific primers (Figure 5B). *INF1*, an elicitin from *Phytophthora infestans* which was reported to require *HSP90* and *SGT1* to trigger cell death (Shibata et al., 2011) was used as a positive control. Remarkably, CC309-mediated cell death was significantly diminished in both *HSP90*- and *SGT1*- silenced plants, compared with TRV-ΔGFP (green fluorescent protein)-silenced plant (Figure 5A). This result

suggests that cell death triggered by overexpression of CC309 occurred through NLR-mediated cell death mechanism.

To corroborate this result, I examined if cell death induced by autoactive G10-NLR or G10-CC domain is similar to HR cell death mediated by expression of an R protein and its cognate effector. Transcript level of defense-related genes were monitored in CC309-, non-autoactive CC10-1-, autoactive full-length *NLR620*- and *Pvr4* with *NIb*-expressing leaves at various time points after agro-infiltration. CC10-1 was included for comparison due to no activation of cell death. Interestingly, overexpression of the autoactive CC309 and *NLR620* resulted in transcript accumulation of cell death marker gene, *Hin1* (Gopalan et al., 1996), and defense-related genes, *PR1*, *WRKY8* and *CYP71D20* (Weitzel and Simonsen, 2015) as observed in expression of *Pvr4* with *NIb* (Figure 6B). However, these genes were not upregulated in leaves expressing CC10-1. These data indicate that cell death induced by autoactive G10-NLR and G10-CC domain may occurr as a consequence of the activation of defense responses similar to the HR.

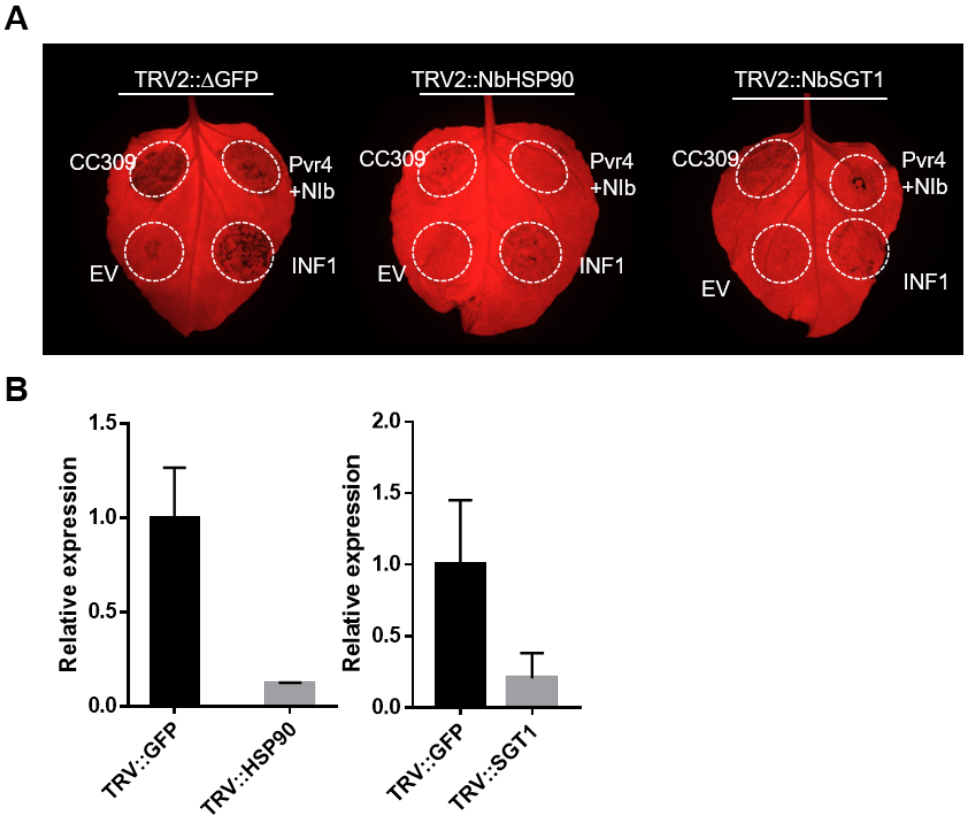

Figure 5. Cell death induced by G10-CC domain is associated with the components of defense-related pathway.

(A) The G10-CC domain-induced cell death was largely decreased in *NbHSP90* and *NbSGT1*-silenced *N. benthamiana*. (B) Silencing efficiency in *NbHSP90* or *NbSGT1*-silenced plants. Two week-old seedlings were infiltrated with *Agrobacteria* carrying TRV-*NbHSP90*, *NbSGT1* or TRV-*GFP* constructs and leaf samples were collected 2 weeks after infiltration. Transcript levels for each gene were analyzed by qRT-PCR using a *NbEF1-a* gene as an internal control.

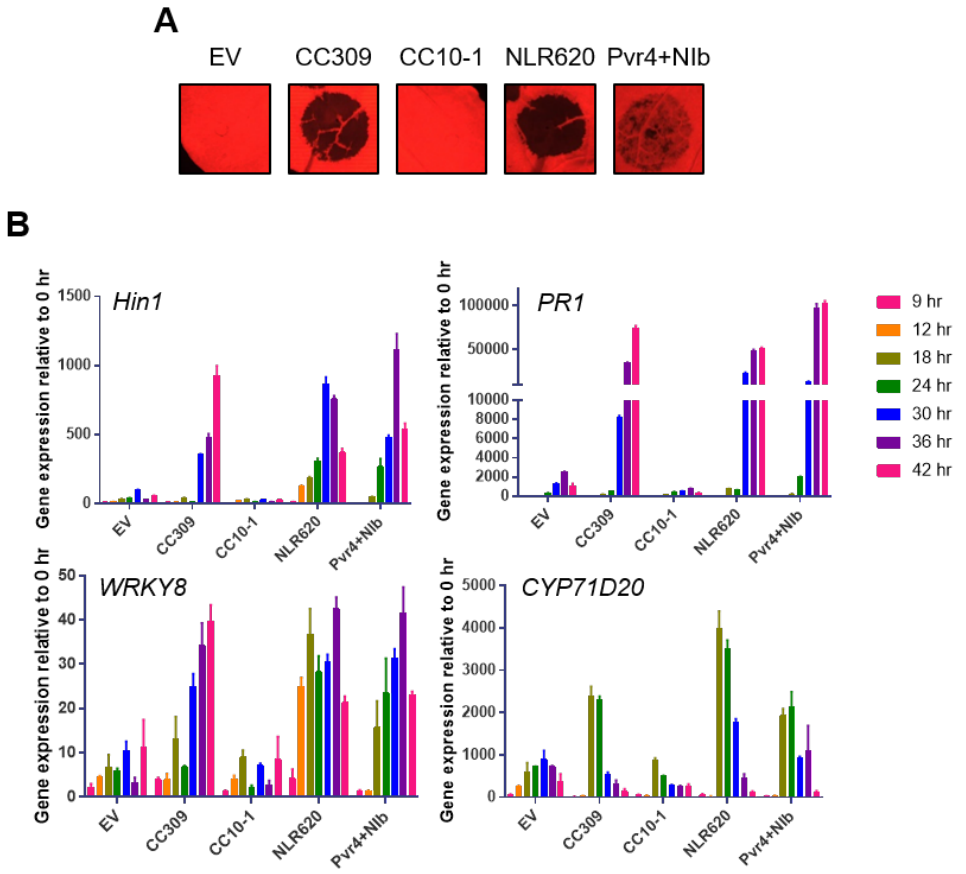

Figure 6. HR- and defense-related genes are up-regulated dramatically in cell death induced by CC309, *NLR620* and *Pvr4* with *NIb* overexpressed leaves. (A) Phenotype of cell death induced by CC309, CC10-1, full-length *NLR620* and *Pvr4* with *NIb*. (B) Relative gene expression for a cell death marker gene *Hin1*, defense response-related genes, *PR1* and *WRKY8,* and a capsidiol biosynthesis gene, *CYP71D20,* was assessed by quantitative reverse transcription polymerase chain reaction (qRT-PCR) at 0, 9, 12, 18, 24, 30, 36, 42 hr after infiltration of Agrobacterium carrying the empty vector, *CC309*, *CC10-1*, *NLR620*, *Pvr4+NIb*. Transcript levels of the analyzed genes were normalized to the levels of the *NbEF1-α* transcript.

The N-terminal motif of G10-CCs is critical for autoactivity

To understand the molecular basis underlying cell death induced by autoactive G10-CC domain, CC309 and CC10-1 were used for further studies. Although these domains share high similarity at the amino acid sequence level (90 % identity), overexpression of the CC309 caused cell death 28~30 hr after agro-infiltration, while expression of the CC10-1 failed to trigger cell death (Figure 7A and 7B). Although transcript level of CC309 and CC10-1 in leaves overexpressing these fragments were similar (Figure 7C), CC10-1 protein accumulated less than CC309 protein. To stabilize CC10-1 protein accumulation, a proteasome inhibitor, MG132, was applied. However, MG132 treatment did not affect protein stability nor cell death-inducing activity of CC10-1. This result suggests that CC10-1 protein is not targeted to proteasome-dependent degradation machinery (Figure 7D).

To identify an essential region for inducing cell death, amino acid sequences of CC10-1 and other autoactive CC domains in the subclade III were aligned (Figure 8A). Compared with other autoactive CC domains, frequent polymorphisms were detected in N-terminal region of CC 10-1, corresponding to 1-12 aa in CC309. To verify these sequence variations are associated with autoactivity, amino acids in 1-12 aa region of CC309 were replaced with corresponding residues of CC10-1. Interestingly, substitution

in 7-12 aa (mCC309$^{7-12}$) and 1-12 aa (mCC309$^{1-12}$) region of CC309, but not substitution in 1-6 aa region (mCC309$^{1-6}$), compromised cell death-inducing the activity (Figure 8B). Immunoblot confirmed the protein accumulation of all variants (Figure 8C).

In addition, substitution of N-terminal region in CC10-1 with 'TAILSP' motif which is a corresponding sequence of 7-12 aa in CC309 slightly acquire cell death-inducing activity (Figure 8D). Furthermore, to see if 'TAILSP' motif affects HR cell death triggered by R protein-effector association, mutations were introduced in both the *Pvr4* and *Pvr4* CC domain, CC322. Transient overexpression in *N. benthamiana* showed that these mutations completely abolished cell death activity of CC domain and full-length *Pvr4* (Figure 9). There results suggest that 'TAILSP' motif at 7-12 aa region in G10-CCs and G10-NLR is critical to trigger cell death.

Next, each amino acid in 'TAILSP' in CC309 was replaced with alanine or glutamate to identify residue responsible for autoactivity. As a result, I7E, L8E and P10A totally abolished autoactivity of CC309 (Figure 10A). Immunoblot confirmed the protein accumulation of all variants (Figure 10B). Ternary structural modeling of the CC309 predicted that these residues might be important to form a α-helix structure and be exposed to the surface (Figure 11). This prediction assumes that N-terminus of G10-CCs may function as an

interface to allow interaction with other components required for inducing cell death. Taken together, these results suggest that ‘TAILSP’ motif at the N-terminal domain of G10-CC domains is crucial for cell death signaling.

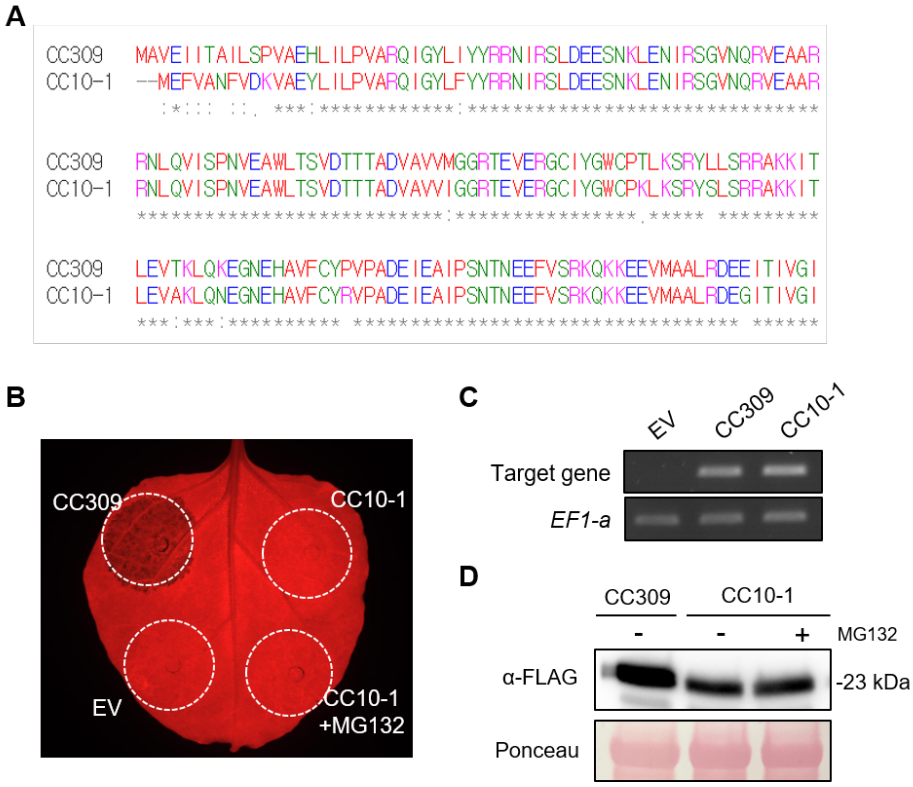

Figure 7. Differential cell death activity of CC309 and CC10-1.
(A) Alignment of amino acid of the CC309 and CC10-1. (B) CC309 and CC10-1 fragments fused to FLAG tag were transiently expressed in *N. benthamiana*. 100 μM MG132 was treated 24 hr after infiltration of *Agrobacterium* carrying CC10-1. Empty vector (EV) were used for negative control. The photograph was taken 3 days post *Agrobacterium* infiltration. (C) Transcripts level of CC309 and CC10-1 were quantified by RT-PCR in the infiltrated leaves. Leaf sectors were collected 26 hr post infiltration. (D) Western blot showing protein expression level of CC309 and CC10-1 in infiltrated leaves. Equal protein loading was confirmed by membrane staining by Ponceau solution.

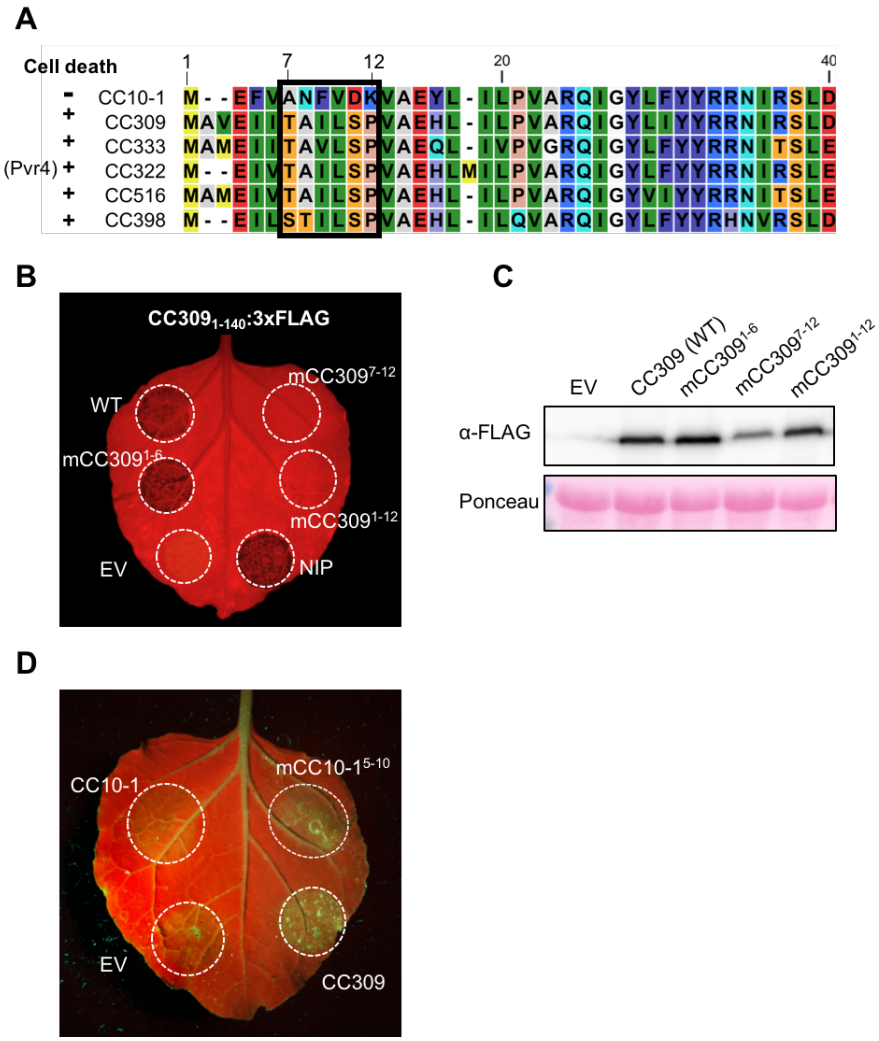

Figure 8. The N-terminal region of G10-CCs is crucial for cell death activity. (A) Alignment of amino acid of the N-termini of clade III in G10-CCs. (B) Amino acids substitution mutation of N-terminal region of CC309 for corresponding region of CC10-1. mCC309$^{1-6}$, 1st to 6th amino acids were replaced; mCC309$^{7-12}$, 7th to 12th amino acids were substituted; mCC309$^{1-12}$,1st to 12th amino acids were replaced. Empty vector (EV) and necrosis-inducing protein (NIP) from *P. sojae* were used for negative control and

positive control, respectively. (C) Total protein was extracted from Agrobacterium-infiltrated tissues and used for western blot to detect the expression level of the fused protein using FLAG antibody. Leaf samples were taken 26 hr post Agrobacterium infiltration. Equal protein loading was confirmed by membrane staining by ponceau solution. (D) CC10-1 and mutated CC10-1 protein fragments were transiently expressed in *N. benthamiana*. The photographs were taken 72 hr after infiltration.

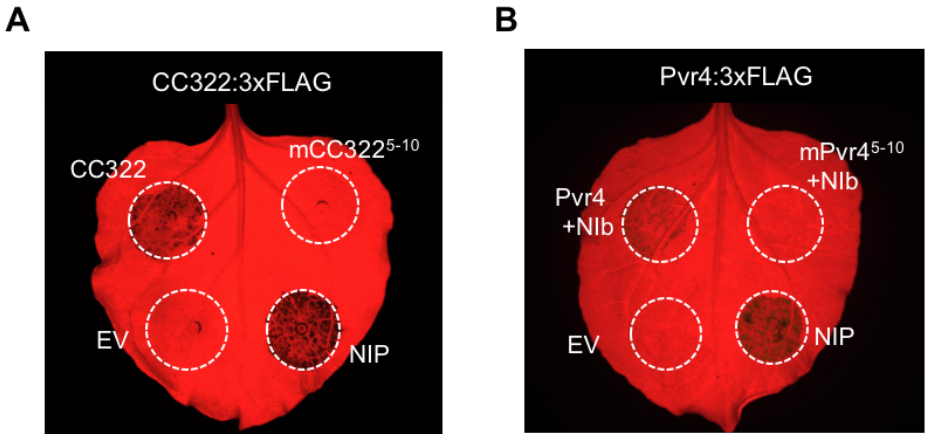

Figure 9. The N-terminal region plays crucial role in induction of HR cell death.
(A) CC322 (CC domain of Pvr4) and mCC322$^{5-10}$, replaced with 5-10 aa region was expressed in *N. benthamiana.* (B) Wild type *Pvr4* and mutated *Pvr4* were co-expressed with NIb of PepMoV. Empty vector (EV) and necrosis-inducing protein (NIP) from *P. sojae* were used for negative control and positive control, respectively. The photographs were taken 72 hr after infiltration.

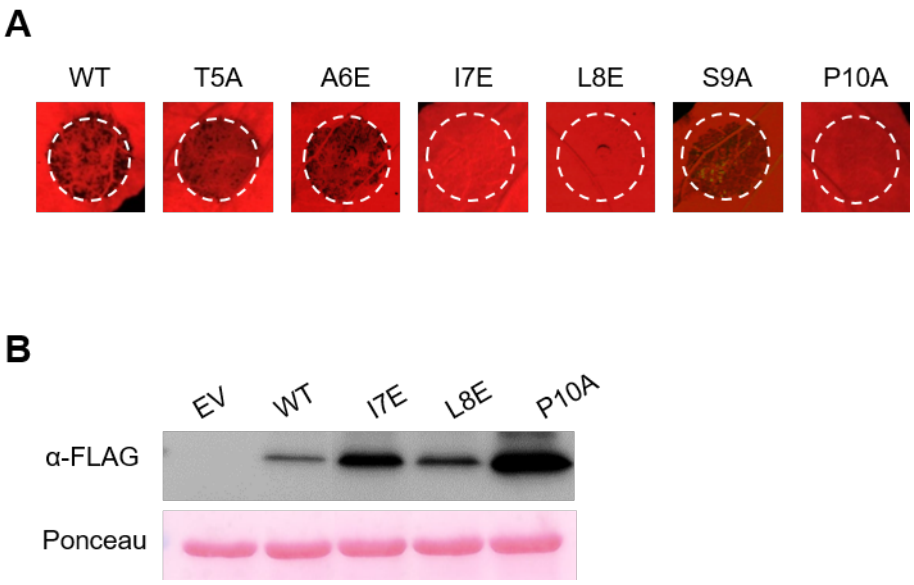

Figure 10. Mutation of leucine, isoleucine and proline residue in N-terminal region of CC309 abolishes cell death-inducing activity.
(A) Each of six amino acids was replaced with alanine or glutamate. (B) Protein accumulation of the CC309 mutants fused to FLAG tag was examined by western blot analysis. Equal protein loading was confirmed by membrane staining by ponceau solution.

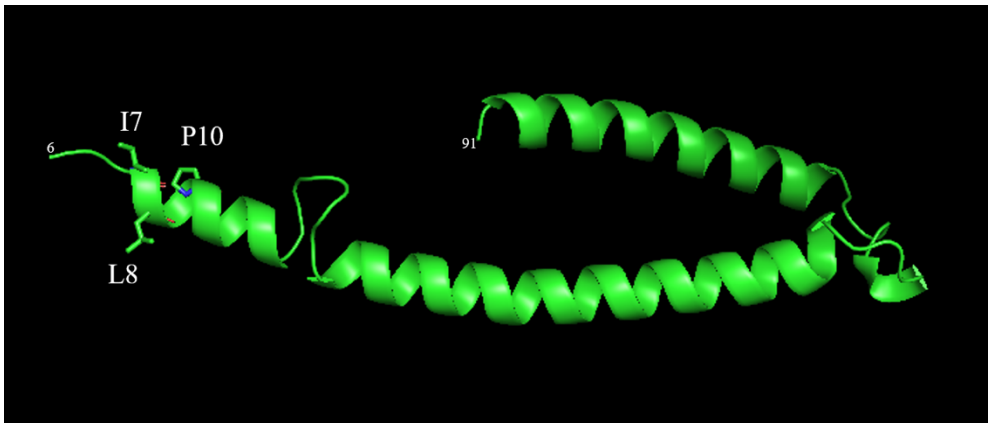

Figure 11. Molecular surface view of the homology model of CC309.
The predicted structure of N-terminal region (6-91 aa) within CC309 was constructed based on the crystal structure of barley MLA10 by SWISS-MODEL program. The side chain of I, L and P residues were present on the surface on the structure.

The 'TAILSP' motif does not affect the localization of G10-CCs

The topology of G10-CCs was predicted using the computer programs such as TMHMM server (http://www.cbs.dtu.dk/services/TMHMM/), TMpred (https://embnet.vital-it.ch/software/TMPRED_form.html) and TMMOD (http://liao.cis.udel.edu/website/servers/TMMOD). TMpred program predicted that G10-CCs contain a transmembrane domain in N-terminus, whereas TMMOD and TMHMM could not predict the transmembrane domain. To confirm the subcellular localization of G10-CCs, N- or C-terminal GFP fusion of G10-CCs were generated. Since tagging of N-terminal GFP to G10-CCs impaired their autoactivity (data not shown), C-terminal GFP fused G10-CCs were used for localization study. The GFP-fused CC309, CC322 and CC10-1 were transiently expressed in *N. benthamiana* and fluorescence was imaged by confocal laser scanning microscopy at 26 hr post infiltration before onset of cell death. GFP signal was observed at the boundary of the cell expressing G10-CCs (Figure 12A). To determine the localization of G10-CCs, FM4-64, membrane-binding fluorescent dye, was applied to the infiltrated leaves (Fischer-Parton et al., 2000). GFP fluorescence for G10-CCs completely merged with FM4-64-labeled signal, suggesting that G10-CCs are localized at the plasma membrane. To more precisely determine subcellular localization, cells

expressing respectively CC309-GFP, CC322-GFP and CC10-1-GFP were plasmolysed following with 1 M NaCl. The cells showed shrinking of the protoplast surrounded by a fluorescent plasma membrane connected to the cell wall by Hechtian strands (Figure 12B).

Because ‘TAILSP’ motif is part of a predicted transmembrane domain, fluorescence of CC10-1-GFP was assumed not to be present at the plasma membrane. However, fluorescence of CC10-1-GFP was also detected at the plasma membrane despite lack of ‘TAILSP’ motif. This result implies that ‘TAILSP’ motif might be not responsible for subcellular localization of G10-CCs to the plasma membrane.

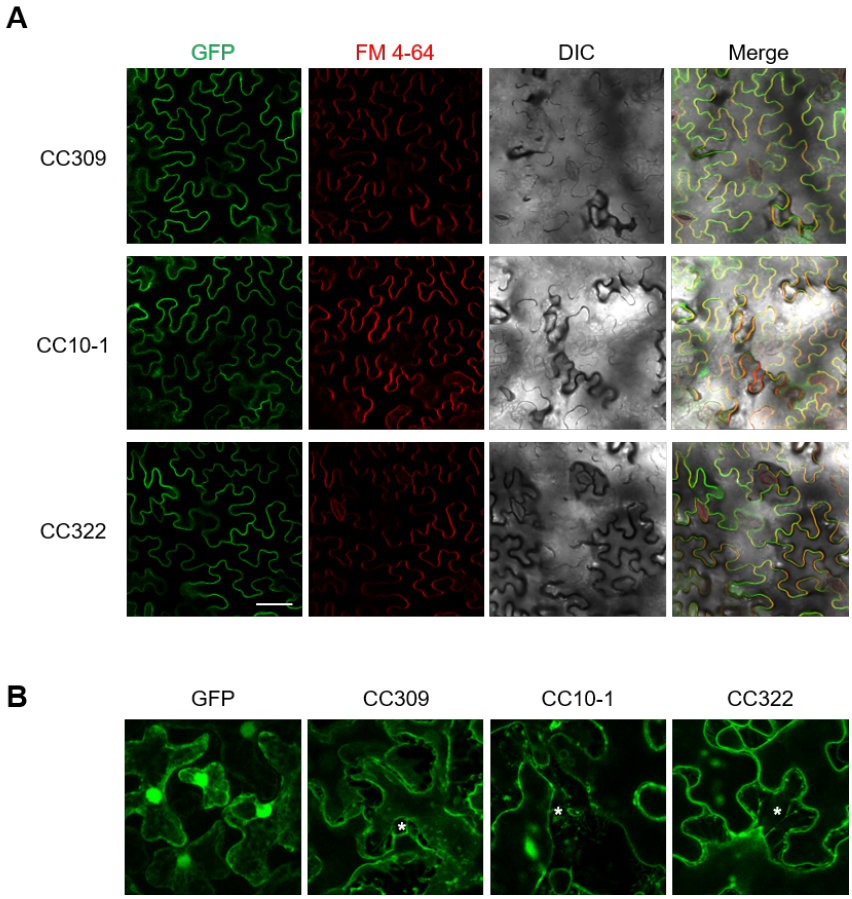

Figure 12. G10-CCs localize at the plasma membrane.
(A) Confocal microscopy image illustrating GFP fused G10-CC domains with the FM4-64 dye at the plasma membrane. Bar=40 μm (B) Plasmolysis of cells carried out by incubating leaf sectors in 1 M NaCl solution. Asterisks indicate Hechtian strands.

Defining minimal region of G10-CC as a signaling module

The G10-CC domains generally contain 4~5 α-helix motifs. In case of CC309, five helixes are present and one coiled-coil structure is predicted (Figure 13A). To define a minimal functional region triggering cell death, N-terminal and C-terminal deletion mutants of CC309 were generated and then expressed in *N. benthamiana* leaves to assess their cell death-inducing activity. C-terminal deletion fragments C1 and C2, but not C3, were still functional (Figure 13B), suggesting that 4 α-helixes are indispensable for autoactivity. To quantify cell death, the leakage of ions caused during cell death was measured in the infiltrated leaves. Interestingly, C2 mutants showed higher activity than C1 mutants (Figure 13C), implying the region from 140 to 165 aa may negatively affect cell death-inducing activity. Moreover, all deletions from the N-terminus (N1, N2 and N3) compromised the autoactivity of CC309 (Figure 13B). These results revealed that the fragment from 1 to 140 aa could be defined as a minimal region of CC309 to induce cell death.

Immunoblot was conducted to verify expression level of all deletion mutants. Since all N-terminal mutants exhibited relatively low stability, I could not exclude the possibility that their malfunction might be resulted from low protein accumulation. To increase stability, all deletion mutants were

fused to the GFP tag which enables further accumulation of small size protein. However, GFP-fused N1, N2, and N3 mutants still showed no activity (Data not shown). Consistent with N-terminal mutation analysis, this result suggests that N-terminus of G10-CC domain is important to induce cell death.

As mentioned before, G10-CCs possess a putative transmembrane domain at N-terminus. To see if the loss of function of all N-terminal deletion mutants is due to improper targeting to the plasma membrane, subcellular localization of these deletion mutants was examined. Unexpectedly, fluorescence signal of all mutants was detected at the plasma membrane regardless of presence of transmembrane domain and their autoactivity (Figure 14). This result suggests that G10-CC domains might be localized at the plasma membrane by interacting with peripheral protein(s). Taken together, N-terminus of G10-CC is important to cell death signaling rather than targeting to the plasma membrane.

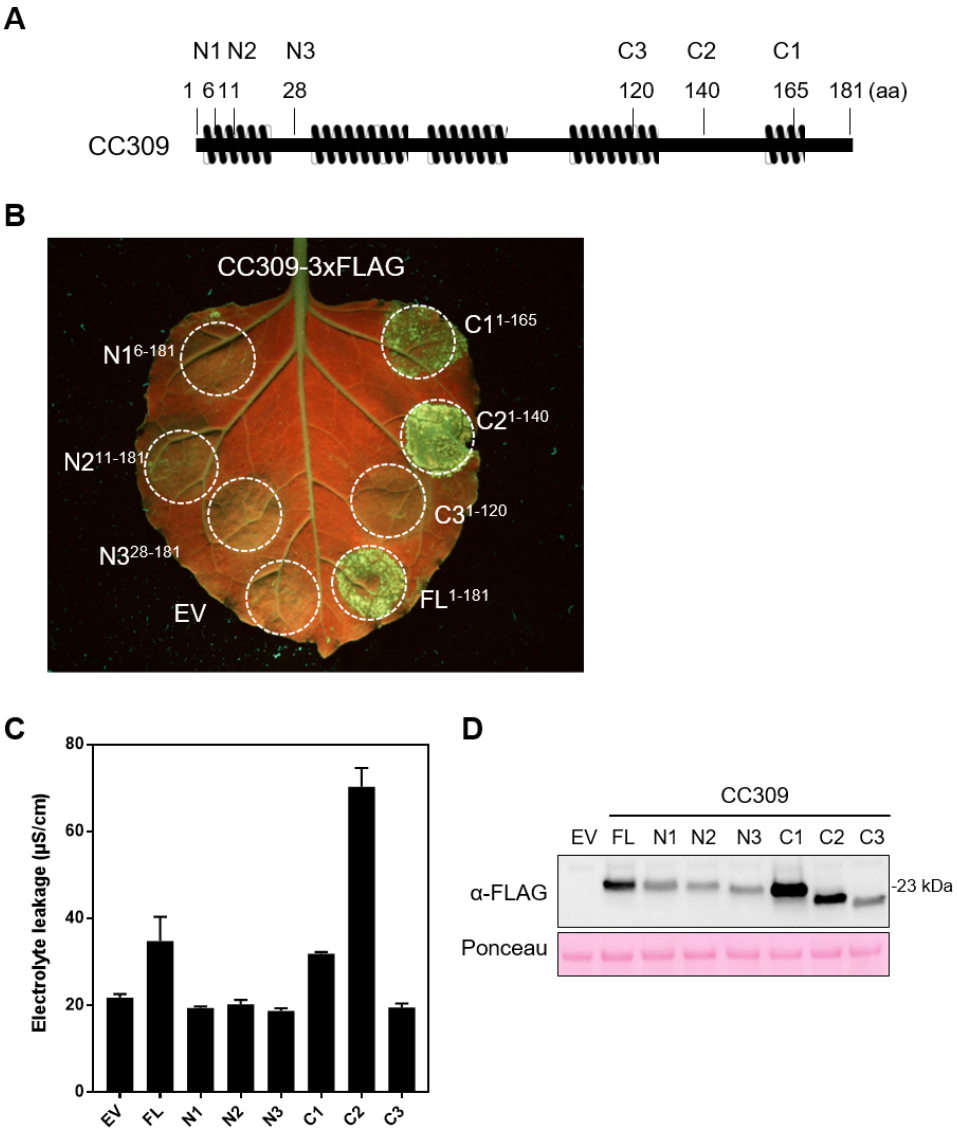

Figure 13. Defining the functional region of CC309.
(A) A schematic diagram of the CC309 showing helix structures and the positions of the deletion mutants used in (B) are shown at the top. (B) Deletion mutants of CC309 were transiently expressed in *N. benthamiana*. (C) Electrolyte leakage was measured at 48 hr post agro-infiltration. Data show average and SD of three replicates. (D) Protein accumulation of the CC309

deletion mutants fused to FLAG tag was examined by western blot analysis. Equal protein loading was confirmed by membrane staining by ponceau solution.

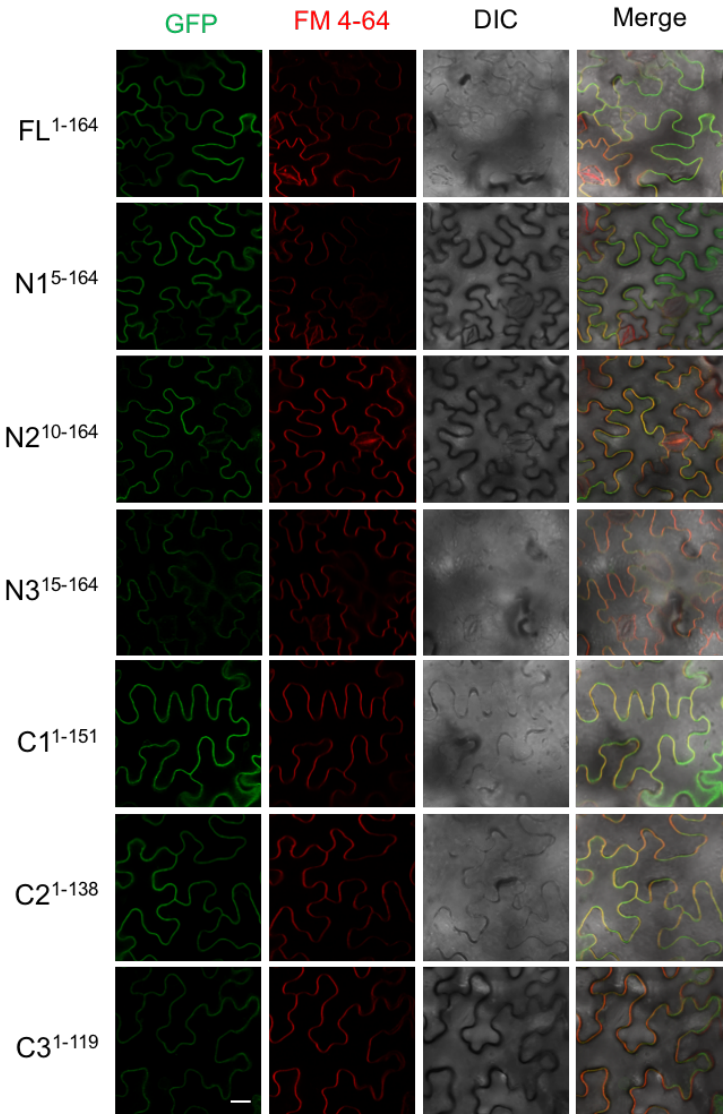

Figure 14. Subcellular localization of deletion mutants of CC309.
Confocal microscopy image illustrating GFP-fused CC309 deletion mutants colocalization with the FM4-64 dye at the plasma membrane. Bar=20 μm

The G10-NLR mediated cell death does not require *EDS1*, *NDR1* and SA-related signaling pathway

NLRs activate downstream signaling components to trigger ROS production, activation of hormone signaling and transcription reprogramming and onset of cell death. In many cases, downstream signaling components of NLR genes are well conserved. Among them, *EDS1* (*Enhanced Disease Susceptibility 1*) and *NDR1* (*Non race-specific Disease Resistance 1*) positively regulate basal immunity against virulent pathogens and known to be important regulators in TNL or CNL-mediated immunity, respectively (Aarts et al., 1998).

In order to examine the genetic components required for G10-CC-triggered cell death, *EDS1* and *NDR1*-silenced *N. benthamiana* plants were used. *EDS1* is known to be a TNL-specific signaling component, however, also contributes to CNL *RPS2*-mediated immunity (Cui et al., 2017). Gene fragments of *EDS1* and *NDR1* were amplified from *N. benthamiana* cDNA, and then cloned into TRV2 vector for VIGS. Although expression levels were significantly reduced in silenced plants (Figure 15B), cell death induced by CC309 and co-expression of *Pvr4* and *NIb* were observed in these gene-silenced plants (Figure 15A). These results suggest that cell death induced by

G10-NLR or G10-CC domain are not associated with EDS1 or NDR-dependent pathway.

However, a typical SA-responsive marker gene, *PR1* was highly upregulated during cell death induced by both G10-NLR and G10-CC domain (Figure 6), implying that SA-related pathway may be associated with G10-NLR-mediated cell death. There are several genes important to the SA signaling. including a SA biosynthesis gene, *Isochorismate synthase 2* (*ICS2*), a SA-signaling component genes, *SA-binding proteins 2* (*SABP2*) which converts methyl SA (inactive) into SA, and *Non-expressor of pathogenesis-related genes 1* (*NPR1*), a transcriptional regulator of SA-mediated systemic acquired resistance. To test SA-signaling pathway is involved in G10-CC-mediated cell death, *ICS2*-, *NPR1*-and *SABP2*-silenced plants were used. Unexpectedly, cell death induced by CC309 and *Pvr4* with *NIb* was significantly enhanced in I*CS2*-, *NPR1*-and *SABP2*-silenced plants compared with TRV-GFP plants (Figure 16A). Silencing efficiency in silenced plants was confirmed by qRT-PCR using gene-specific primers (Figure 16B). To further confirm that endogenous SA level affects the G10-CC-mediated cell death, transgenic plants expressing the bacterial *NahG* gene which encodes salicylate hydroxylase that degrades SA, were examined. *NahG* transgenic plants accumulate very little SA and are defective to systemic acquired

resistance (SAR) (Delaney et al., 1994). As observed in *ICS2*-, *NPR1*-and *SABP2*-silenced plants, cell death caused by the G10-CC domain was enhanced in *NahG* transgenic plants (Figure 17A). To quantify cell death, the leakage of ions caused during cell death was measured in the infiltrated site (Figure 17B). Interestingly, *ICS2, SABP2* and *NPR1*-silenced plants also showed accelerated cell death induced by *INF1*-mediated cell death. Since both *ICS2* and *SABP2* gene are involved in synthesis of SA and production of active SA respectively, low accumulation of SA might affect the virulence of *Agrobacterium*, which results in increasing the expression level of G10-CCs. Indeed, *ICS2-, NPR1-*, and *SABP2*-silenced *N. benthamiana* was reported to exhibit the increased susceptibility to *Agrobacterium* (Anand et al., 2008). While *ICS2-, NPR1-*, and *SABP2*-silencing enabled significant reduction in transcript level of these genes compared to the *GFP*-silenced plant, these silenced plants did not lose the ability to mount cell death in response to G10-NLR and G10-CC domain. These data suggest that cell death induced by G10-NLR or G10-CC domain was not associated with SA-signaling pathway.

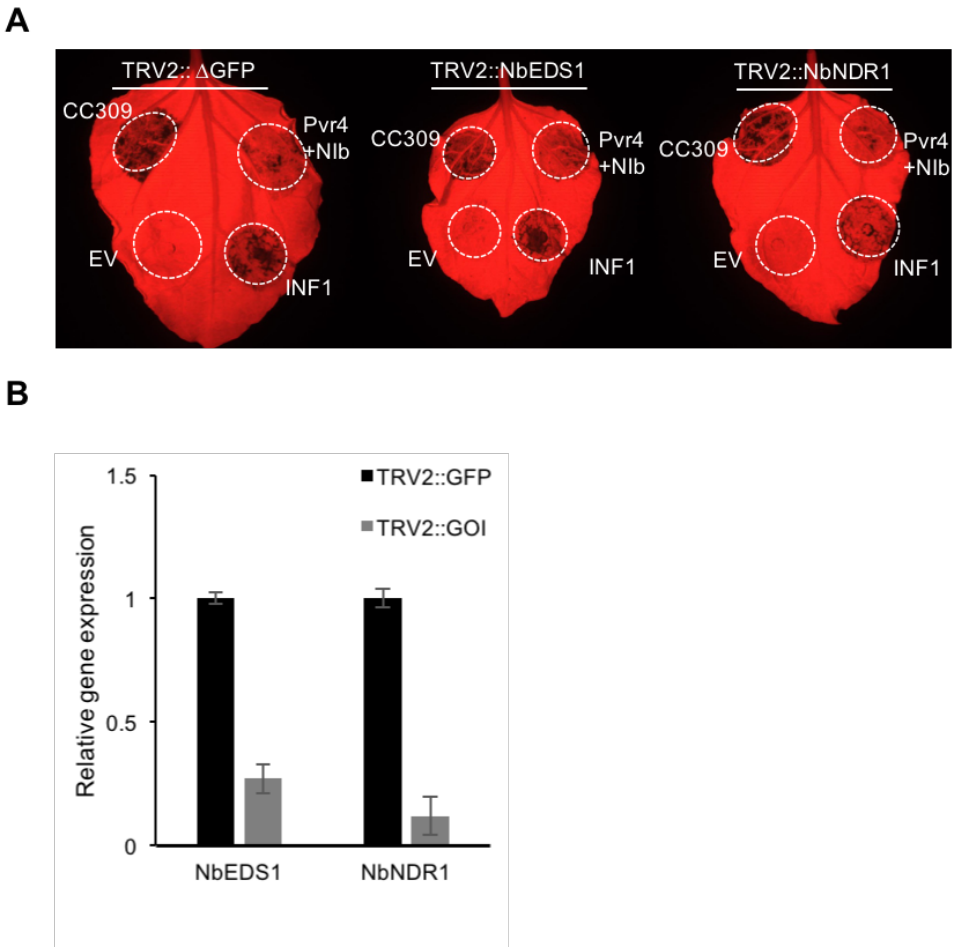

Figure 15. Cell death induced by G10-CC or G10-NLR does not require *EDS1* and *NDR1*.

Agrobacterium carrying CC309 and Pvr4 with NIb were transiently infiltrated in *NbEDS1* and *NbNDR1*-silenced *N. benthamiana*. The photographs were taken 72 hr after infiltration. (B) Silencing efficiency in *NbEDS1* and *NbNDR1*-silenced plants. Samples were collected 2 weeks after Agroinfiltration. Transcript level for each gene were analyzed by qRT-PCR using a *NbEF1-a* gene as an internal control.

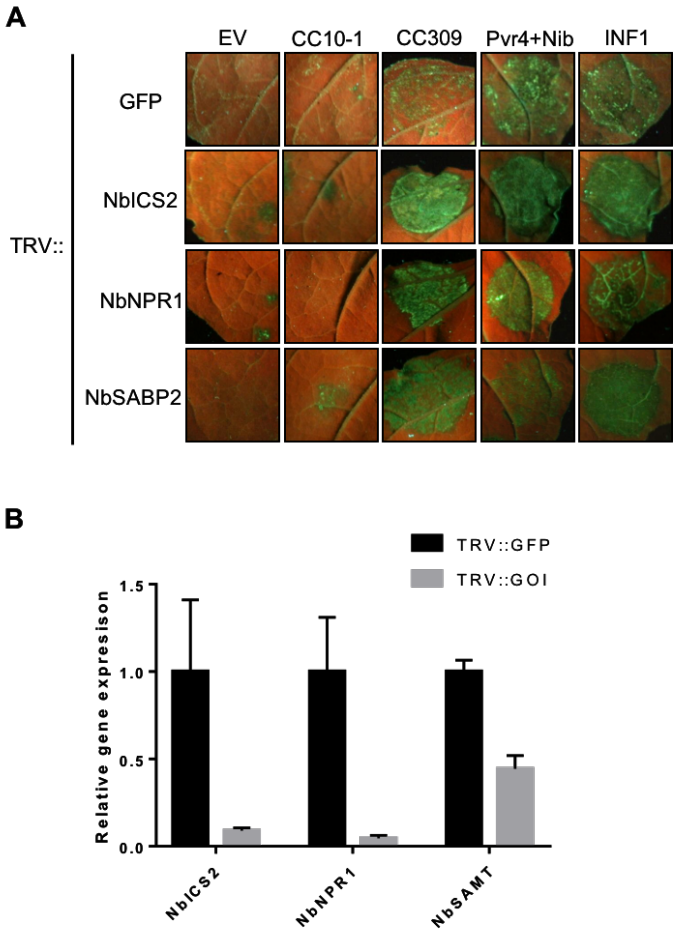

Figure 16. Cell death induced by G10-CC domain or G10-NLR is enhanced in salicylic acid biosynthesis or signaling related genes-silenced plants.
(A) Agrobacterium carrying G10-CC domain and G10-NLR were transiently infiltrated in *NbICS2, NbNPR1* or *NbSABP2*-silenced *N. benthamiana*. (B) Silencing efficiency in *NbICS2, NbNPR1* or *NbSABP2*-silenced plants. Samples were collected 2 weeks after Agroinfiltration. Transcript level for each gene were analyzed by qRT-PCR using a *NbEF1-a* gene as an internal control.

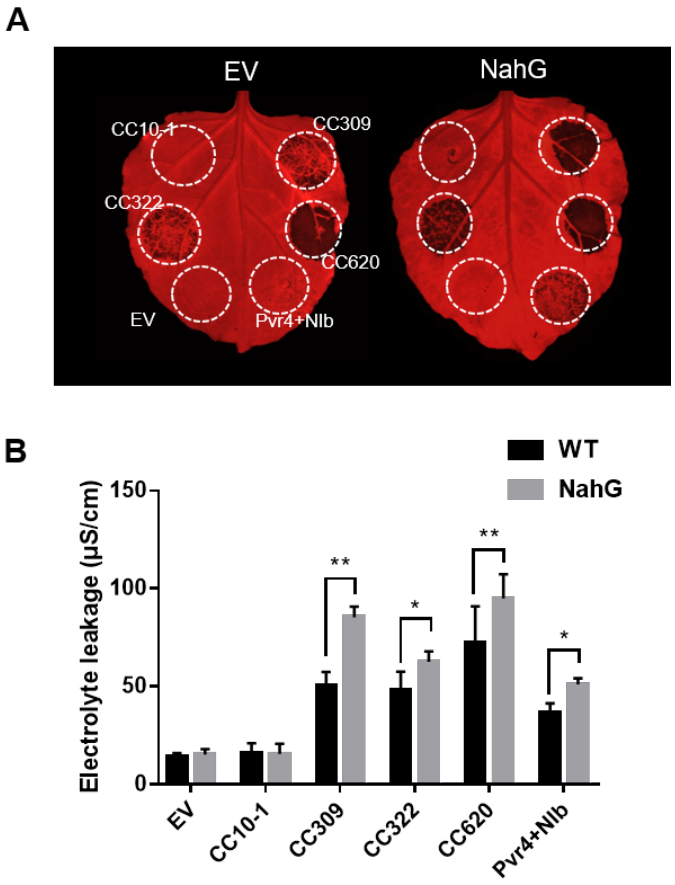

Figure 17. Cell death induced by G10-CC domain or G10-NLR is enhanced in *NahG* transgenic plant.
(A) G10-CC domains and G10-NLRs were transiently expressed in WT and *NahG* transgenic plant. The photograph was taken 48 hr post infiltration. (B) Electrolyte leakage was measured at 30 hr post infiltration. Data show average and SD of three replicates.

SAHH is a candidate interacting protein of G10-CCs

To better understand the molecular basis of cell death of G10-CCs, protein pull down assay was performed to identify binding partners of G10-CCs in the *N. benthamiana* expressing 3xFLAG-tagged CC309 protein (Table 2). Unexpectedly, most of candidate proteins were predicted to be localized to chloroplast, even though CC309 were localized at the plasma membrane. For further study, S-adenosyl homocysteine hydrolase (SAHH) was chosen, because the peptides of SAHH were detected in duplicate IP (immunoprecipitation) samples and cytoplasmic SAHH was expected to be likely to interact with plasma membrane-localized CC309 (Lee et al., 2012).

SAHH is a key enzyme in cycle to synthesis of S-adenosyl-methionine (SAM), which donates its methyl group to numerous methylation reactions. Li et al., 2015 reported that expression of tomato *SAHH* genes is induced by virulent bacterial pathogen, *Pseudomonas syringae* pv. *Tomato* (*Pst*) DC3000 and by the hormones such as SA, JA and precursor of ethylene in tomato. Moreover, *SAHH*-silenced tomato plants exhibited increased SA level and enhanced resistance to *Pst* DC3000.

There are three copies of the *SAHH* genes in *N. benthamiana* genome and two of them were detected by LC-MS/MS analysis. To test if *N. benthamiana* SAHHs are also involved in defense responses, two *NbSAHH* genes were

silenced in *N. benthamiana* using VIGS system. Silencing of *NbSAHHs* resulted in inhibition of developmental growth with aberrant leaf expansion showing an epinastic phenotype (Figure 18A). Additionally, the leaves of *NbSAHH*-silenced plant became wilted and some death spot was exhibited on the silenced leaves. To explore the involvement of these phenotypes in defense responses, accumulation of ROS in *NbSAHH*-silenced plants was examined by DAB staining. Compared with control plants, H_2O_2 accumulation was observed in *SAHH*-silenced plants without any inoculation of pathogen (Figure 18B). These data suggest that inactivation of *SAHH*s might induce constitutive activation of immune responses.

To assess the effect of *SAHH* on the G10-CC domain-mediated cell death, C-terminal GFP-tagged *SAHH* and CC309 were co-expressed in *N. benthamiana*. When *Agrobacterium* contacting SAHH-GFP and CC309 were co-infiltrated in *N. benthamiana*, CC309-mediated cell death was slightly decreased in infiltrated leaves. The possibility was considered that CC309 rapidly induced cell death before *SAHH* had not been sufficiently expressed or fully maturated to function properly. To rule out this possibility, *Agrobacterium* harboring CC309 was infiltrated 4 hr after transient expression of *SAHH* or *GFP* alone by agroinfiltration. In contrast with GFP, cell death triggered by CC309 was clearly compromised by co-expression

with SAHH-GFP (Figure 19A). In addition, cell death induced by CC322 (the CC domain of Pvr4) or *Pvr4* with *NIb* was also affected co-expression with *SAHH* in *N. benthamiana* (Figure 19B). However, cell death induced by *INF1* was not affected by co-expression of *SAHH*. These results suggest that *SAHH* may be involved in the G10-NLR mediated cell death, but not *INF1*-mediated cell death in *N. benthamiana*.

However, it is necessary to confirm that the G10-CC domain directly interacts with SAHHs and how the G10-CC domain regulates the activity of SAHH. Nonetheless, these results suggest that SAHH may function as a repressor of cell death induced by G10-CC domain and G10-NLRs and serve as a potential target of G10-CC domain to trigger cell death.

Table 3. Candidate proteins identified as interactor proteins with CC309

reference	Gene Symbol/Annotation	Localization prediction	MW(kDa)	PSM*								Sum intensity*				Test IP:Control IP	Test IP:Control IP/ MW
				Unique eGFP #1	Total eGFP_#1	Unique eGFP #2	Total eGFP_#2	Unique CC309_#1	Total CC309_#1	Unique CC309_#2	Total CC309_#2	Sum Intensity eGFP_#1	Sum Intensity eGFP_#2	Sum Intensity CC309_#1	Sum Intensity CC309_#2		
CC309			23000	0	0	0	0	6	166	7	57	1.00E+00	1.00E+00	3.70E+09	2.80E+08	995000000	43261
GFP			26869	27	987	29	1352	0	0	0	0	6.00E+10	2.50E+11	1.00E+00	1.00E+00	0	0
NbS00015312g0005.1	WrbA_quinone reductase	Plastid	25559	0	0	0	0	0	0	8	47	1.00E+00	1.00E+00	1.00E+00	2.90E+07	7250000	284
NbS00002207g0005.1	WrbA_quinone reductase	Plastid	20397	0	0	0	0	0	0	6	41	1.00E+00	1.00E+00	1.00E+00	2.10E+07	5250000	257
NbS00040464g0006.1	WrbA_quinone reductase	Plastid	21576	0	0	0	0	0	0	4	20	1.00E+00	1.00E+00	1.00E+00	1.80E+07	4500000	209
NbS00028438g0001.1	Thioredoxin M precursor	Plastid	12885	0	0	0	0	1	1	4	13	1.00E+00	1.00E+00	4.20E+04	7.60E+06	1910500	148
NbS00014241g0002.1	AtpA_ATP synthase subunit α	Plastid	21833	0	0	0	0	1	3	1	4	1.00E+00	1.00E+00	3.90E+06	1.70E+06	1400000	64
NbS00056676g0007.1	WrbA_quinone reductase	Plastid	13891	0	0	0	0	0	0	1	5	1.00E+00	1.00E+00	1.00E+00	3.10E+06	775000	56
NbS00019029g0008.1	APX1	Plastid	27448	0	0	0	0	1	8	8	32	1.00E+00	1.00E+00	3.80E+05	5.20E+06	1395000	51

	_Ascorbate peroxidase																
NbS00018155g0020.1	Glyoxylate reductase	Cytosol	50719	0	0	0	0	0	0	2	3	1.00E+00	1.00E+00	1.00E+00	9.00E+06	2250000	44
NbS00026910g0004.1	Nucleoside diphosphate kinase 1	Mitochondria	16288	0	0	0	0	0	0	5	12	1.00E+00	1.00E+00	1.00E+00	2.70E+06	675000	41
NbS00053747g0002.1	SAHH _S-adenosyl homosystein hydrolase	Cytosol	10537	0	0	0	0	1	2	1	4	1.00E+00	1.00E+00	1.10E+05	1.50E+06	402500	38
NbS00008945g0004.1	Pyruvate kinase	Cytosol /Chloroplast	57368	0	0	0	0	0	0	14	36	1.00E+00	1.00E+00	1.00E+00	6.70E+06	1675000	29
NbS00010360g0001.1	AtpA _ATP synthase subunit α	Plastid	10741	0	0	0	0	1	3	1	2	1.00E+00	1.00E+00	1.00E+06	2.00E+05	300000	28
NbS00038282g0004.1	PSAN _Photosystem I reaction centre subunit N ";	Plastid	18046	0	0	0	0	0	0	1	3	1.00E+00	1.00E+00	1.00E+00	1.90E+06	475000	26
NbS00016819g0006.1	CYP20-1 _cyclophilin-like protein	Unknown	26379	0	0	0	0	0	0	1	6	1.00E+00	1.00E+00	1.00E+00	2.30E+06	575000	22
NbS00035717g0012.1	PRXQ _PeroxiredoxinQ	Plastid	23572	0	0	0	0	0	0	2	6	1.00E+00	1.00E+00	1.00E+00	2.00E+06	500000	21
NbS00009002g0109.1	UGP_ glucose-1-phosphate uridylyltransferase	Plastid	43052	0	0	0	0	1	1	12	30	1.00E+00	1.00E+00	2.40E+04	3.60E+06	906000	21
NbS00001322g0010.1	AtpA _ATP synthase subunit α	Plastid	35443	0	0	0	0	2	4	2	3	1.00E+00	1.00E+00	1.90E+06	7.90E+05	672500	19

NbS00033013g0010.1	UPTG2_Alpha-1 4-glucan-protein synthase	Plastid	44207	0	0	0	0	2	2	3	9	1.00E+00	1.00E+00	7.20E+04	3.20E+06	818000	19
NbS00014507g0009.1	PRXIIF_Peroxiredoxin 2F	Plastid	20957	0	0	0	0	0	0	2	6	1.00E+00	1.00E+00	1.00E+00	1.50E+06	375000	18
NbS00042478g0005.1	SHMT_Serine hydroxyl methyltransferase	Unknown	57324	0	0	0	0	1	3	6	22	1.00E+00	1.00E+00	1.50E+05	3.70E+06	962500	17
NbS00054073g0003.1	PRXIIC_Peroxiredoxin 2C	Plastid	13942	0	0	0	0	1	1	3	7	1.00E+00	1.00E+00	1.30E+04	8.80E+05	223250	16
NbS00018070g0006.1	AtpE_ATP synthase CF1 epsilon subunit	Plastid	8814	0	0	0	0	2	4	1	3	1.00E+00	1.00E+00	2.90E+05	2.30E+05	130000	15
NbS00003479g0020.1	COMT_catechol O-methyltransferase	Unknown	39715	0	0	0	0	2	4	2	7	1.00E+00	1.00E+00	1.30E+05	2.10E+06	557500	14
NbS00025946g0006.1	AtpF__ATP synthase subunit I	Plastid	11207	0	0	0	0	2	5	1	2	1.00E+00	1.00E+00	5.80E+05	4.80E+04	157000	14
NbS00060910g0004.1	PRXQ_PeroxiredoxinQ	Plastid	22999	0	0	0	0	0	0	4	10	1.00E+00	1.00E+00	1.00E+00	1.20E+06	300000	13
NbS00005125g0015.1	Glycolate oxidase	Plastid	38806	0	0	0	0	0	0	7	15	1.00E+00	1.00E+00	1.00E+00	2.00E+06	500000	13
NbS00013149g0011.1	PRO3_Profilin 3	Unknown	14455	0	0	0	0	0	0	1	4	1.00E+00	1.00E+00	1.00E+00	7.20E+05	180000	12
NbS00011498g0005.1	THF1_Thylakoid formation 1	Plastid	17161	0	0	0	0	0	0	1	1	1.00E+00	1.00E+00	1.00E+00	8.20E+05	205000	12

NbS00017897g0003.1	Unknown	Unknown	13135	0	0	0	0	0	0	1	3	1.00E+00	1.00E+00	1.00E+00	6.20E+05	155000	12
NbS00017162g0026.1	Peptidyl-prolyl cis-trans isomerase	Unknown	23463	0	0	0	0	0	0	5	18	1.00E+00	1.00E+00	1.00E+00	1.10E+06	275000	12
NbS00028134g0008.1	Eif3ja_Translation initiation factor eIF3 subunit	Nucleus	25161	0	0	0	0	2	5	4	8	1.00E+00	1.00E+00	4.60E+05	6.60E+05	280000	11
NbS00035350g0004.1	Pyruvate kinase	Cytosol/Chloroplast	14890	0	0	0	0	0	0	2	8	1.00E+00	1.00E+00	1.00E+00	6.40E+05	160000	11
NbS00027882g0011.1	LAPA2_Leucine aminopeptidase	Cytosol/Chloroplast	60648	0	0	0	0	0	0	15	45	1.00E+00	1.00E+00	1.00E+00	2.60E+06	650000	11
NbS00004640g0017.1	Pyruvate kinase	Cytosol/Chloroplast	49776	0	0	0	0	1	3	8	19	1.00E+00	1.00E+00	1.80E+04	2.10E+06	529500	11
NbS00009456g0023.1	CLEB3J9_Ascorbate peroxidase	Plastid	39656	0	0	0	0	1	2	5	9	1.00E+00	1.00E+00	3.50E+04	1.50E+06	383750	10
NbS00001892g0060.1	SOD_Manganese/iron superoxide dismutase	Mitochondria	25987	0	0	0	0	1	2	1	3	1.00E+00	1.00E+00	5.60E+04	9.40E+05	249000	10

*: Peptide-spectrum match

**: Sum intensity of peptide areas for a given protein

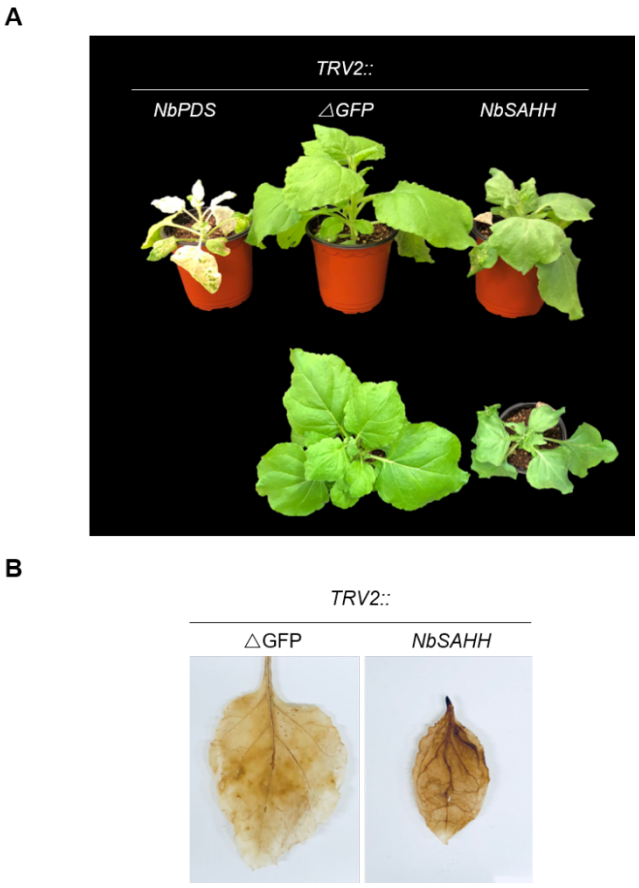

Figure 18. *NbSAHH*-silenced plants exhibit inhibition of growth and enhanced H_2O_2 accumulation.
(A) Silencing of *NbSAHH*s inhibited developmental growth with the aberrant leaf expansion showing an epinastic phenotype.
(B) Leaves of silenced plants were stained with diaminobenzidine (DAB) to visualize accumulation of hydrogen peroxide.

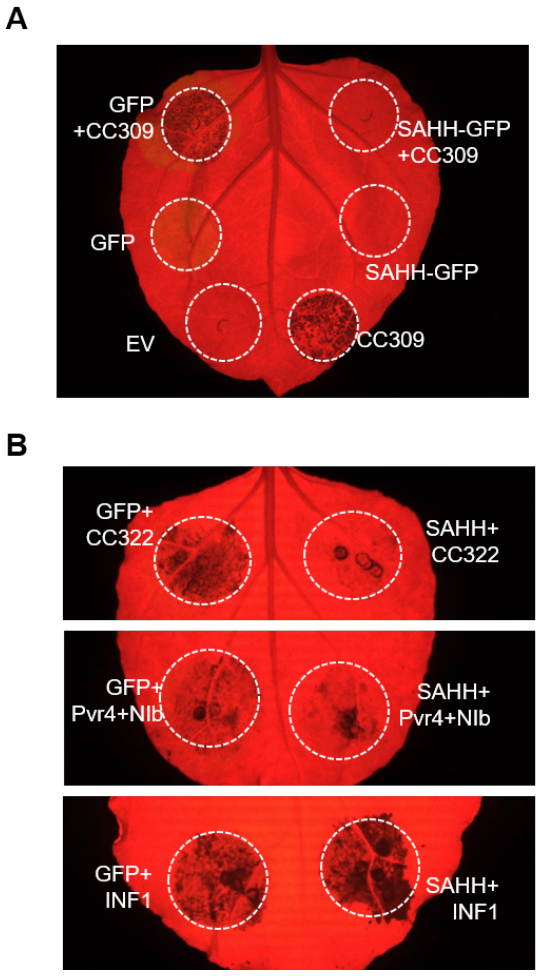

Figure 19. *NbSAHH* impairs cell death induced by G10-CC domain and G10-NLR.

Transient expression of *GFP* and *SAHH-GFP* were followed 4 hr later by infiltration of *Agrobacterium* carrying CC309 (A), CC322, *Pvr4* with *NIb* and *INF1* (B). Photos were taken 48 hr after agroinfiltration.

CHAPTER V. DISCUSSION

Distinct role of G10-NLRs in plant immunity

Screening for pepper autoactive NLR revealed that 16 out of 415 NLRs induced cell death when overexpressed in *N. benthamiana* (Table 2). Among them, only two and three autoactive NLR genes in GT and G10 respectively, contain an autoactive N-terminal domain, whereas none of N-terminal domains of autoactive NLRs in the other groups induced cell death. Similarly, although overexpression of the full-length *Arabidopsis RPS2* and *RPS5* induced HR-like cell death in absence of the corresponding effectors, expression of the CC-NB domain, not the CC domain alone, induces cell death (Day et al., 2005; Ade et al., 2007). In this cases, the CC domains of RPS2 and RPS5 seemed not to be sufficient for cell death induction. Moreover, overexpression of NB domain of potato Rx resistance protein induces HR-like cell death, suggesting that other subdomains in NLR also has the property to trigger cell death signaling. Therefore, these observations indicate that NLR protein might transduce a downstream signaling in diverse way.

Recently, transient overexpression of the CC domains from *I2*-like genes in tomato and tobacco was reported to induce cell death in *N. benthamiana,* but never with the CC domains of the pepper *I2*-like NLRs (Hamel et al., 2016). Interestingly, fusion of the enhanced yellow fluorescent protein (YFP) to the C-terminal of CC domain of pepper *I2*-like NLRs (note that the pepper *I2*-like NLRs belong to G4) trigger strong cell death upon transient overexpression in *N. benthamiana*. This tag-dependent autoactivity has been observed in several CC domains of NLRs regardless of the level of protein accumulation (Wang et al., 2015). The GFP and YFP are known to have a weak dimerization tendency, which might have affected the activity of CC domain to induce cell death. Since cell death activity of N-terminal domain with no tag was screened in this study, the G4-CC domains in pepper were not identified.

G10-NLRs have different features from typical CNLs. Most of the CNL-type functional R proteins contain the conserved 'EDVID' motif in their CC domain and disruption of this motif compromised disease resistance (Rairdan et al., 2008). However, like CC_R type NLRs, G10-CC domain lacks 'EDVID' motif which plays an important role in intramolecular interaction with NB-ARC or LRR domain and intermolecular interaction (Rairdan et al., 2008). In addition, phylogenetic tree constructed by NLRs from 3 pepper species

(*Capsicum annuum, C. baccatum and C. chinense*), tomato, potato and rice revealed that G10-NLRs was branched out from typical CNL groups and closely related to TNLs and CC_R group (Figure 20). NRG1 and ADR1, members of CC_R-NLR group, are evolutionally ancient and conserved in angiosperm (Collier et al., 2011b). Recently, these genes have been known to function as 'helper' NLRs required for some NLR-mediated resistance. Moreover, transient overexpression of their CC_R domains is sufficient to induce HR responses. Taken together, these findings opened up the possibility that G10-NLRs may have a distinct role in plant immunity especially in terms of cell death.

Downstream signaling of G10-NLR mediated cell death

Downstream signaling components for ETI are well conserved. Among them, molecular chaperone components, *HSP90* and *SGT1* are essential for proper folding and accumulation of NLRs. Previously, it was shown that *Pvr4*-mediated HR cell death was abolished in *SGT1*- and *HSP90*- silenced plants (Kim et al., 2018). As expected, cell death induced by overexpression of G10-CC was also compromised in *HSP90*- and *SGT1*-silenced plants (Figure 6). Thus, both cell death induced by G10-NLR with effector and G10-CC alone requires *SGT1* and *HSP90* to initiate the defense signaling.

To investigate more essential component of G10-NLR signaling, cell death induced by G10-NLR or G10-CC was examined in plants where transcription level of SA signaling genes, and defense signaling hub genes (*EDS1* and *NDR1*) were reduced by VIGS. Unexpectedly, G10-NLR mediated cell death was not affected these genes (Figure 15 and 16). These results can be explained by a functional redundancy. Especially, redundancy between *EDS1* and *NDR1* disease resistance pathways were reported in *Arabidopsis RPP7*- and *RPP8*-mediated immunity against the oomycete pathogen *Hyaloperonospora arabidopsidis* (McDowell et al., 2000). Moreover, cell death induced by G10-NLRs did not seemed to require accumulation of SA, though SA-responsive gene *PR1* was highly expressed during induction of cell death by G10-NLR or G10-CC domain (Figure 17). These results implied G10-NLR-mediated cell death is not associated with SA accumulation and may require others yet undiscovered signaling component of immune signaling.

Potential role for SAHH in the regulation of HR cell death

SAHH is a key enzyme hat catalyzes the hydrolysis of S-adenosyl homocysteine (SAH) to adenosine and L-homocysteine in transmethylation reactions. Homocystein is converted to methionine, a precursor of S-

adenosylmethionine (SAM) which is an important molecule involved in various biological reactions including 5' end cap methylation, polyamine biosynthesis, methionine salvation cycle and ethylene biosynthesis (De et al., 2018). SAHH acts to recycle the SAH in methionine synthesis cycle. Given that a large set of methyl acceptor compounds such as nucleic acids, lipids and cell wall components in the cell, knock-out of some genes involved in this cycle results in developmental abnormalities or completely sterile. Actually, mutations of *Arabidopsis methionine adenosyltransferase 4* (*MAT4)*, which encodes SAM synthase and *Arabidopsis SAHH1* are embryo-lethal, indicating these SAM cycle genes are essential genes in plant (Rocha et al., 2005; Meng et al., 2018).

In this study, SAHH was screened out as a candidate protein interacting with the G10-CC domain by the protein pull-down experiment with LC-MS/MS analysis. Since the by-products from SAM cycle are involved in numerous reactions in the cell, it is not easy to definitely explain how SAHH will associate with cell death induced by G10-NLR or G10-CC. However, the following scenario can be proposed to explain the possible roles of SAHH in HR-like cell death.

The G10-NLR or G10-CC mediated cell death was almost completely abrogated by co-expression of SAHH in *N. benthamiana.* This result

demonstrated that SAHH act as a negative regulator of cell death induced by G10-CC or G10-NLR. G10-CC may lead to inactivation of SAHH protein by regulating the protein stability or blocking the active sites of this enzyme. The inactivation of SAHH may then build up the cellular environment to be favorable for cell death. Previous reports showing that *SAHH* knock-down plants exhibited enhanced defense responses corroborated this hypothesis (Li et al. 2015). Transgenic plant with low expression level of *SAHH* showed a pleiotropic phenotype including developmental abnormalities and hypomethylation of DNA (Tanaka et al., 1997). Genome-wide analysis of gene expression pattern in *Arabidopsis SAHH1* mutant revealed that a subset of gene transcripts was up-regulated (Jordan et al., 2007). Many of the differential expressed genes were mapped to pathways essential to plant growth and development including those of primary, secondary and hormone metabolisms (Ouyang et al., 2012). However, it is difficult to conclude that global expression change by hypomethylation of DNA directly causes cell death.

The second aspect is a ROS accumulation. ROS functions as 'redox messengers' to trigger programmed cell death in plant. SAHH-silenced plant showed increased accumulation of H_2O_2 (Figure 18B), indicating that SAHH functions as a negative regulator for ROS accumulation. Recently, De *et al*.,

2018 presented that *SAM synthase* and *SAHH* silencing caused a significant reduction in glutathione level in PVX-infected plants (De et al., 2018). Glutathione is oxidized by ROS and functions as an antioxidant agent that prevents excessive oxidation of sensitive cellular components (Noctor et al., 2012). At present, it is not clear how disruption of methylation biosynthesis pathway can affect glutathione concentration. In animal and fungi, reverse-transsulfuration enzyme which catalyzed homocysteine to cysteine and glutathione biosynthesis is present whereas that enzyme could not be detected in plant and bacteria. It was, however, reported that plants possess an alternative to the reverse-transsulfuration pathway via methanethiol (Goyer et al., 2007), supporting that methionine pathway could have an effect on glutathione biosynthesis by regulating biosynthesis of cysteine, a precursor of glutathione. To address this hypothesis, further study is necessary to verify if inactivation of SAHH actually links to reduction of glutathione level and ROS accumulation.

The third scenario is high accumulation of cytokinins. Previously, SAHH was found to be present in a cytokinin-binding protein complex purified from tobacco leaves, thus SAHH was proposed to be a cytokinin-binding protein (Mitsui et al., 1993). It was also reported that partial loss-of function mutation of the *Arabidopsis SAHH1* gene and antisense of tobacco *SAHH* resulted in

accumulation of cytokinins (Masuta et al., 1995; Li et al., 2008). It can be assumed that reduction of SAHH amount resulted in increase in the number of free active cytokinin molecules. Moreover, plants overexpressing cytokinin synthesis gene, *Arabidopsis isopentenyltransferase* (*ipt*) developed necrotic lesion and severe wilting as similar to the phenotype of *SAHH*-silenced *N. benthamiana* (Figure 18A). These evidences indicate the possibility that cytokine mediates cell death induced by G10-NLR or G10-CC.

Several scenarios were proposed to explain how SAHH affects to mediate cell death induced by G10-NLR. However, more experiments need to be conducted to prove these hypotheses. Above all, direct evidence demonstrating the interaction between SAHH and G10-CCs should be presented in order to establish molecular mechanism underlying G10-NLR mediated cell death.

In this study, molecular mechanism in which G10-NLR or G10-CC domains induce HR-like cell death was examined. Autoactive G10-CC domains are suitable materials to study how NLRs trigger HR cell death, a most extreme type of plant defense responses. The results in this study will provide the clues to understand the distinct role of G10-NLRs in plant immunity.

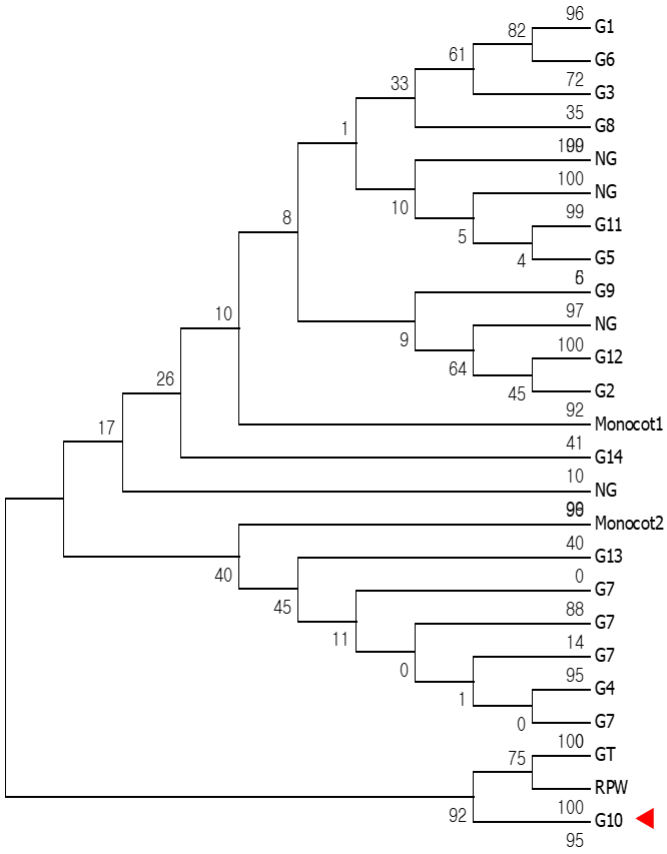

Figure 20. Phylogenetic tree of NLRs in six plant species.
All NB-ARC domains of NLRs in pepper (*Capsicum annuum*, *C. baccatum* and *C. chinense*), tomato, potato and rice were used for the phylogenetic relationship analysis. This phylogenetic tree was constructed by a neighbor-joining method with MEGA6. Subgroups were classified into 17 groups according to Seo et al., 2016.

REFERENCES

Aarts, N., Metz, M., Holub, E., Staskawicz, B.J., Daniels, M.J., and Parker, J.E. (1998). Different requirements for *EDS1* and *NDR1* by disease resistance genes define at least two R gene-mediated signaling pathways in *Arabidopsis*. Proc Natl Acad Sci U S A **95,** 10306-10311.

Abramovitch, R.B., Kim, Y.J., Chen, S.R., Dickman, M.B., and Martin, G.B. (2003). *Pseudomonas* type III effector AvrPtoB induces plant disease susceptibility by inhibition of host programmed cell death. Embo J **22,** 60-69.

Ade, J., DeYoung, B.J., Golstein, C., and Innes, R.W. (2007). Indirect activation of a plant nucleotide binding site-leucine-rich repeat protein by a bacterial protease. Proc Natl Acad Sci U S A **104,** 2531-2536.

Anand, A., Rojas, C.M., Tang, Y.H., and Mysore, K.S. (2012). Several components of SKP1/Cullin/F-box E3 ubiquitin ligase complex and associated factors play a role in *Agrobacterium*-mediated plant transformation. New Phytol **195,** 203-216.

Anand, A., Uppalapati, S.R., Ryu, C.M., Allen, S.N., Kang, L., Tang, Y., and Mysore, K.S. (2008). Salicylic acid and systemic acquired resistance play a role in attenuating crown gall disease caused by *Agrobacterium tumefaciens*. Plant Physiol **146,** 703-715.

Arasimowicz-Jelonek, M., Floryszak-Wieczorek, J., Gzyl, J., and Chmielowska-Bak, J. (2013). Homocysteine over-accumulation as the effect of potato leaves exposure to biotic stress. Plant Physiol

Biochem **63,** 177-184.

Aslanidis, C., and de Jong, P.J. (1990). Ligation-independent cloning of PCR products (LIC-PCR). Nucleic Acids Res **18,** 6069-6074.

Austin, M.J., Muskett, P., Kahn, K., Feys, B.J., Jones, J.D.G., and Parker, J.E. (2002). Regulatory role of *SGT1* in early R gene-mediated plant defenses. Science **295,** 2077-2080.

Bai, S., Liu, J., Chang, C., Zhang, L., Maekawa, T., Wang, Q., Xiao, W., Liu, Y., Chai, J., Takken, F.L., Schulze-Lefert, P., and Shen, Q.H. (2012). Structure-function analysis of barley NLR immune receptor MLA10 reveals its cell compartment specific activity in cell death and disease resistance. PLoS Pathog **8,** e1002752.

Bendahmane, A. (2003). Constitutive gain-of-function mutants in a nucleotide binding site-leucine rich repeat protein encoded at the *Rx* locus of potato. Plant J **33,** 603-603.

Bernoux, M., Ve, T., Williams, S., Warren, C., Hatters, D., Valkov, E., Zhang, X., Ellis, J.G., Kobe, B., and Dodds, P.N. (2011). Structural and functional analysis of a plant resistance protein TIR domain reveals interfaces for self-association, signaling, and autoregulation. Cell Host Microbe **9,** 200-211.

Bonardi, V., Tang, S.J., Stallmann, A., Roberts, M., Cherkis, K., and Dangl, J.L. (2011). Expanded functions for a family of plant intracellular immune receptors beyond specific recognition of pathogen effectors. Proc Natl Acad Sci U S A **108,** 16463-16468.

Bos, J.I.B., Chaparro-Garcia, A., Quesada-Ocampo, L.M., Gardener, B.B.M., and Kamoun, S. (2009). Distinct amino acids of the *Phytophthora infestans* effector AVR3a condition activation of R3a hypersensitivity and suppression of cell death. Mol Plant Microbe

Interact **22,** 269-281.

Burch-Smith, T.M., Schiff, M., Caplan, J.L., Tsao, J., Czymmek, K., and Dinesh-Kumar, S.P. (2007). A novel role for the TIR domain in association with pathogen-derived elicitors. PLoS Biol **5,** 501-514.

Casey, L.W., Lavrencic, P., Bentham, A.R., Cesari, S., Ericsson, D.J., Croll, T., Turk, D., Anderson, P.A., Mark, A.E., Dodds, P.N., Mobli, M., Kobe, B., and Williams, S.J. (2016). The CC domain structure from the wheat stem rust resistance protein Sr33 challenges paradigms for dimerization in plant NLR proteins. Proc Natl Acad Sci U S A **113,** 12856-12861.

Century, K.S., Holub, E.B., and Staskawicz, B.J. (1995). *Ndr1*, a locus of *Arabidopsis thaliana* that is required for disease resistance to both a bacterial and a fungal pathogen. Proc Natl Acad Sci U S A **92,** 6597-6601.

Cesari, S., Moore, J., Chen, C., Webb, D., Periyannan, S., Mago, R., Bernoux, M., Lagudah, E.S., and Dodds, P.N. (2016). Cytosolic activation of cell death and stem rust resistance by cereal MLA-family CC-NLR proteins. Proc Natl Acad Sci U S A **113,** 10204-10209.

Cesari, S., Kanzaki, H., Fujiwara, T., Bernoux, M., Chalvon, V., Kawano, Y., Shimamoto, K., Dodds, P., Terauchi, R., and Kroj, T. (2014). The NB-LRR proteins RGA4 and RGA5 interact functionally and physically to confer disease resistance. Embo J **33,** 1941-1959.

Chae, E., Bomblies, K., Kim, S.T., Karelina, D., Zaidem, M., Ossowski, S., Martin-Pizarro, C., Laitinen, R.A., Rowan, B.A., Tenenboim, H., Lechner, S., Demar, M., Habring-Muller, A., Lanz, C., Ratsch, G., and Weigel, D. (2014). Species-wide genetic incompatibility analysis identifies immune genes as hot spots of deleterious epistasis.

Cell **159,** 1341-1351.

Chen, X.J., Zhu, M., Jiang, L., Zhao, W.Y., Li, J., Wu, J.Y., Li, C., Bai, B.H., Lu, G., Chen, H.Y., Moffett, P., and Tao, X.R. (2016). A multilayered regulatory mechanism for the autoinhibition and activation of a plant CC-NB-LRR resistance protein with an extra N-terminal domain. New Phytol **212,** 161-175.

Chiarini, F., and Bernardello, G. (2006). Karyotype studies in South American species of *Solanum* subgen. *Leptostemonum* (Solanaceae). Plant Biol **8,** 486-493.

Coll, N.S., Epple, P., and Dangl, J.L. (2011). Programmed cell death in the plant immune system. Cell Death Differ **18,** 1247-1256.

Collier, S.M., Hamel, L.P., and Moffett, P. (2011). Cell death mediated by the N-terminal domains of a unique and highly conserved class of NB-LRR protein. Mol Plant Microbe Interact **24,** 918-931.

Cook, D.E., Mesarich, C.H., and Thomma, B.P.H.J. (2015). Understanding plant immunity as a surveillance system to detect invasion. Annu Rev Phytopathol **53**, 541-563.

Cui, H., Gobbato, E., Kracher, B., Qiu, J., Bautor, J., & Parker, J. E. (2017). A core function of EDS1 with PAD4 is to protect the salicylic acid defense sector in *Arabidopsis* immunity. New Phytol **213**, 1802-1817.

Day, B., Dahlbeck, D., Huang, J., Chisholm, S.T., Li, D., and Staskawicz, B.J. (2005). Molecular basis for the RIN4 negative regulation of RPS2 disease resistance. Plant Cell **17,** 1292-1305.

De, S., Chavez-Calvillo, G., Wahlsten, M., and Makinen, K. (2018). Disruption of the methionine cycle and reduced cellular gluthathione levels underlie potex-potyvirus synergism in *Nicotiana benthamiana*.

Mol Plant Pathol **19,** 1820-1835.

Delaney, T. P., Uknes, S., Vernooij, B., Friedrich, L., Weymann, K., Negrotto, D., and Ryals, J. (1994). A central role of salicylic acid in plant disease resistance. Science, **266**, 1247-1250.

Dodds, P.N., and Rathjen, J.P. (2010). Plant immunity: towards an integrated view of plant-pathogen interactions. Nat Rev Genet **11,** 539-548.

Dong, Y., Burch-Smith, T.M., Liu, Y., Mamillapalli, P., and Dinesh-Kumar, S.P. (2007). A ligation-independent cloning tobacco rattle virus vector for high-throughput virus-induced gene silencing identifies roles for *NbMADS4*-1 and -*2* in floral development. Plant Physiol **145,** 1161-1170.

Ellis, J.G., Lawrence, G.J., Luck, J.E., and Dodds, P.N. (1999). Identification of regions in alleles of the flax rust resistance gene *L* that determine differences in gene-for-gene specificity. Plant Cell **11,** 495-506.

Fischer-Parton, S., Parton, R.M., Hickey, P.C., Dijksterhuis, J., Atkinson, H.A., and Read, N.D. (2000). Confocal microscopy of FM4-64 as a tool for analysing endocytosis and vesicle trafficking in living fungal hyphae. J Microsc **198**, 246-259

Frost, D., Way, H., Howles, P., Luck, J., Manners, J., Hardham, A., Finnegan, J., and Ellis, J. (2004). Tobacco transgenic for the flax rust resistance gene *L* expresses allele-specific activation of defense responses. Mol Plant Microbe Interact **17,** 224-232.

Gao, Z.Y., Chung, E.H., Eitas, T.K., and Dang, J.L. (2011). Plant intracellular innate immune receptor Resistance to *Pseudomonas syringae* pv. *maculicola 1* (*RPM1*) is activated at, and functions on,

the plasma membrane. Proc Natl Acad Sci U S A **108,** 8915-8915.

Gopalan, S., Wei, W., and He, S.Y. (1996). *hrp* gene-dependent induction of *hin1*: A plant gene activated rapidly by both harpins and the *avrPto* gene-mediated signal. Plant J **10**, 591-600.

Goyer, A., Collakova, E., Shachar-Hill, Y., and Hanson, A.D. (2007). Functional characterization of a methionine gammalyase in *Arabidopsis* and its implication in an alternative to the reverse transsulfuration pathway. Plant Cell Physiol **48,** 232-242.

Guo, M., Tian, F., Wamboldt, Y., and Alfano, J.R. (2009). The Majority of the type III effector inventory of *Pseudomonas syringae* pv. *tomato* DC3000 can suppress plant immunity. Mol Plant Microbe Interact **22,** 1069-1080.

Hamel, L.P., Sekine, K.T., Wallon, T., Sugiwaka, Y., Kobayashi, K., and Moffett, P. (2016). The chloroplastic protein THF1 interacts with the coiled-coil domain of the disease resistance protein N' and regulates light-dependent cell death. Plant Physiol **171,** 658-674.

Heath, M.C. (2000). Nonhost resistance and nonspecific plant defenses. Curr Opin Plant Biol **3,** 315-319.

Heese, A., Hann, D.R., Gimenez-Ibanez, S., Jones, A.M.E., He, K., Li, J., Schroeder, J.I., Peck, S.C., and Rathjen, J.P. (2007). The receptor-like kinase SERK3/BAK1 is a central regulator of innate immunity in plants. Proc Natl Acad Sci U S A **104,** 12217-12222.

Heidrich, K., Tsuda, K., Blanvillain-Baufume, S., Wirthmueller, L., Bautor, J., and Parker, J.E. (2013). *Arabidopsis* TNL-WRKY domain receptor RRS1 contributes to temperature-conditioned RPS4 autoimmunity. Front Plant Sci **4,** 403.

Heil, M., and Baldwin, I.T. (2002). Fitness costs of induced resistance:

emerging experimental support for a slippery concept. Trends Plant Sci **7,** 61-67.

Howles, P., Lawrence, G., Finnegan, J., McFadden, H., Ayliffe, M., Dodds, P., and Ellis, J. (2005). Autoactive alleles of the flax *L6* rust resistance gene induce non-race-specific rust resistance associated with the hypersensitive response. Mol Plant Microbe Interact **18,** 570-582.

Jia, Y., McAdams, S.A., Bryan, G.T., Hershey, H.P., and Valent, B. (2000). Direct interaction of resistance gene and avirulence gene products confers rice blast resistance. Embo J **19,** 4004-4014.

Jones, J.D.G., and Dangl, J.L. (2006). The plant immune system. Nature **444,** 323-329.

Jordan, N.D., West, J.P., Bottley, A., Sheikh, M., and Furner, I. (2007). Transcript profiling of the hypomethylated *hog1* mutant of *Arabidopsis*. Plant Mol Biol **65,** 571-586.

Jurkowski, G.I., Smith, R.K., Yu, I.C., Ham, J.H., Sharma, S.B., Klessig, D.F., Fengler, K.A., and Bent, A.F. (2004). *Arabidopsis DND2*, a second cyclic nucleotide-gated ion channel gene for which mutation causes the "defense, no death" phenotype. Mol Plant Microbe Interact **17,** 511-520.

Kadota, Y., Shirasu, K., and Guerois, R. (2010). NLR sensors meet at the SGT1-HSP90 crossroad. Trends Biochem Sci **35,** 199-207.

Karasov, T.L., Chae, E., Herman, J.J., and Bergelson, J. (2017). Mechanisms to mitigate the trade-off between growth and defense. Plant Cell **29,** 666-680.

Kim, S.B., Lee, H.Y., Seo, S., Lee, J.H., and Choi, D. (2015). RNA-dependent RNA polymerase (NIb) of the *Potyviruses* is an avirulence

factor for the broad-spectrum resistance gene *Pvr4* in *Capsicum annuum* cv. CM334. PLoS One **10,** e0119639.

Kim, S.B., Lee, H.Y., Choi, E.H., Park, E., Kim, J.H., Moon, K.B., Kim, H.S., and Choi, D. (2018). The coiled-coil and leucine-rich repeat domain of the *Potyvirus* resistance protein Pvr4 has a distinct role in signaling and pathogen recognition. Mol Plant Microbe Interact **31,** 906-913.

Kim, S.B., Kang, W.H., Huy, H.N., Yeom, S.I., An, J.T., Kim, S., Kang, M.Y., Kim, H.J., Jo, Y.D., Ha, Y., Choi, D., and Kang, B.C. (2017). Divergent evolution of multiple virus-resistance genes from a progenitor in *Capsicum* spp. New Phytol **213,** 886-899.

Kim, M.S., Kim, S., Jeon, J., Kim, K.T., Lee, H.A., Lee, H.Y., and Choi D. (2018). Global gene expression profiling for fruit organs and pathogen infections in the pepper, *Capsicum annuum* L. Sci data, **5,** 180103.

Krasileva, K.V., Dahlbeck, D., and Staskawicz, B.J. (2010). Activation of an *Arabidopsis* resistance protein is specified by the in planta association of its leucine-rich repeat domain with the cognate oomycete effector. Plant Cell **22,** 2444-2458.

Lee, S., Doxey, A. C., McConkey, B. J., & Moffatt, B. A. (2012). Nuclear targeting of methyl-recycling enzymes in *Arabidopsis thaliana* is mediated by specific protein interactions. Mol Plant **5**, 231-248.

Leister, R.T., Dahlbeck, D., Day, B., Li, Y., Chesnokova, O., and Staskawicz, B.J. (2005). Molecular genetic evidence for the role of *SGT1* in the intramolecular complementation of Bs2 protein activity in *Nicotiana benthamiana*. Plant Cell **17,** 1268-1278.

Li, C.H., Yu, N., Jiang, S.M., Shangguan, X.X., Wang, L.J., and Chen,

X.Y. (2008). Down-regulation of S-adenosyl-L-homocysteine hydrolase reveals a role of cytokinin in promoting transmethylation reactions. Planta **228,** 125-136.

Li, L., Ye, C.F., Zhao, R., Li, X., Liu, W.Z., Wu, F.F., Yan, J.L., Jiang, Y.Q., and Yang, B. (2015). Mitogen-activated protein kinase kinase kinase (MAPKKK) 4 from rapeseed (*Brassica napus* L.) is a novel member inducing ROS accumulation and cell death. Biochem Bioph Res Co **467,** 792-797.

Liu, Y.L., Burch-Smith, T., Schiff, M., Feng, S.H., and Dinesh-Kumar, S.P. (2004). Molecular chaperone Hsp90 associates with resistance protein and its signaling proteins SGT1 and Rar1 to modulate an innate immune response in plants. J Biol Chem **279,** 2101-2108.

Longstaff, M., Brigneti, G., Boccard, F., Chapman, S., and Baulcombe, D. (1993). Extreme resistance to *potato virus X* infection in plants expressing a modified component of the putative viral replicase . Embo J **12,** 2230-2230.

Mackey, D., Holt, B.F., 3rd, Wiig, A., and Dangl, J.L. (2002). RIN4 interacts with Pseudomonas syringae type III effector molecules and is required for RPM1-mediated resistance in *Arabidopsis*. Cell **108,** 743-754.

Mackey, D., Belkhadir, Y., Alonso, J.M., Ecker, J.R., and Dangl, J.L. (2003). *Arabidopsis* RIN4 is a target of the type III virulence effector AvrRpt2 and modulates RPS2-mediated resistance. Cell **112,** 379-389.

Maekawa, T., Cheng, W., Spiridon, L.N., Toller, A., Lukasik, E., Saijo, Y., Liu, P., Shen, Q.H., Micluta, M.A., Somssich, I.E., Takken, F.L.W., Petrescu, A.J., Chai, J., and Schulze-Lefert, P. (2011). Coiled-coil domain-dependent homodimerization of intracellular barley immune

receptors defines a minimal functional module for triggering cell death. Cell Host Microbe **9,** 187-199.

Masuta, C., Tanaka, H., Uehara, K., Kuwata, S., Koiwai, A., and Noma, M. (1995). Broad resistance to plant viruses in transgenic plants conferred by antisense inhibition of a host gene essential in S-adenosylmethionine-dependent transmethylation reactions. Proc Natl Acad Sci U S A **92,** 6117-6121.

McDowell, J.M., Cuzick, A., Can, C., Beynon, J., Dangl, J.L., and Holub, E.B. (2000). Downy mildew (*Peronospora parasitica*) resistance genes in *Arabidopsis* vary in functional requirements for *NDR1*, *EDS1, NPR1* and salicylic acid accumulation. Plant J **22,** 523-529.

Meng, J., Wang, L., Wang, J., Zhao, X., Cheng, J., Yu, W., Jin, D., Li, Q., and Gong, Z. (2018). Methionine adenosyltransferase 4 mediates DNA and histone methylation. Plant Physiol **177,** 652-670.

Mestre, P., and Baulcombe, D.C. (2006). Elicitor-mediated oligomerization of the tobacco N disease resistance protein. Plant Cell **18,** 491-501.

Meyers, B.C., Kozik, A., Griego, A., Kuang, H., and Michelmore, R.W. (2003). Genome-wide analysis of NBS-LRR-encoding genes in *Arabidopsis*. Plant Cell **15,** 809-834.

Meyers, B.C., Dickerman, A.W., Michelmore, R.W., Sivaramakrishnan, S., Sobral, B.W., and Young, N.D. (1999). Plant disease resistance genes encode members of an ancient and diverse protein family within the nucleotide-binding superfamily. Plant J **20,** 317-332.

Mitsui, S., Wakasugi, T., and Sugiura, M. (1993). A cdna-encoding the 57 Kda subunit of a cytokinin-binding protein complex from tobacco - the subunit has high homology to S-adenosyl-L-homocysteine hydrolase. Plant Cell Physiol **34,** 1089-1096.

Moffett, P., Farnham, G., Peart, J., and Baulcombe, D.C. (2002). Interaction between domains of a plant NBS-LRR protein in disease resistance-related cell death. Embo J **21,** 4511-4519.

Moon, J.Y., Lee, J.H., Oh, C.S., Kang, H.G., and Park, J.M. (2016). Endoplasmic reticulum stress responses function in the *HRT*-mediated hypersensitive response in *Nicotiana benthamiana*. Mol Plant Pathol **17,** 1382-1397.

Mucyn, T.S., Clemente, A., Andriotis, V.M.E., Balmuth, A.L., Oldroyd, G.E.D., Staskawicz, B.J., and Rathjen, J.P. (2006). The tomato NBARC-LRR protein Prf interacts with Pto kinase in vivo to regulate specific plant immunity. Plant Cell **18,** 2792-2806.

Mur, L.A.J., Bi, Y.M., Darby, R.M., Firek, S., and Draper, J. (1997). Compromising early salicylic acid accumulation delays the hypersensitive response and increases viral dispersal during lesion establishment in *TMV*-infected tobacco. Plant J **12,** 1113-1126.

Noctor, G., Mhamdi, A., Chaouch, S., Han, Y., Neukermans, J., Marquez-Garcia, B., Queval, G., and Foyer, C.H. (2012). Glutathione in plants: an integrated overview. Plant Cell Environ **35,** 454-484.

Oh, S.K., Kim, S.B., Yeom, S.I., Lee, H.A., and Choi, D. (2010). Positive-selection and ligation-independent cloning vectors for large scale in planta expression for plant functional genomics. Mol Cells **30,** 557-562.

Ouyang, B., Fei, Z.J., Joung, J.G., Kolenovsky, A., Koh, C.S., Nowak, J., Caplan, A., Keller, W.A., Cui, Y.H., Cutler, A.J., and Tsang, E.W.T. (2012). Transcriptome profiling and methyl homeostasis of an *Arabidopsis* mutant deficient in S-adenosylhomocysteine hydrolase1 (*SAHH1*). Plant Mol Biol **79,** 315-331.

Peart, J.R., Mestre, P., Lu, R., Malcuit, I., and Baulcombe, D.C. (2005). NRG1, a CC-NB-LRR protein, together with N, a TIR-NB-LRR protein, mediates resistance against tobacco mosaic virus. Curr Biol **15,** 968-973.

Qi, D., and Innes, R.W. (2013). Recent advances in plant NLR structure, function, localization, and signaling. Front Immunol **4,** 348.

Qi, D., DeYoung, B.J., and Innes, R.W. (2012). Structure-function analysis of the coiled-coil and leucine-rich repeat domains of the RPS5 disease resistance protein. Plant Physiol **158,** 1819-1832.

Raaymakers, T.M., and Van den Ackerveken, G. (2016). Extracellular recognition of oomycetes during biotrophic infection of plants. Front Plant Sci **7,** 906.

Rairdan, G.J., and Moffett, P. (2006). Distinct domains in the ARC region of the potato resistance protein Rx mediate LRR binding and inhibition of activation. Plant Cell **18,** 2082-2093.

Rairdan, G.J., Collier, S.M., Sacco, M.A., Baldwin, T.T., Boettrich, T., and Moffett, P. (2008). The coiled-coil and nucleotide binding domains of the Potato Rx disease resistance protein function in pathogen recognition and signaling. Plant Cell **20,** 739-751.

Reape, T.J., Molony, E.M., and McCabe, P.F. (2008). Programmed cell death in plants: distinguishing between different modes. J Exp Bot **59,** 435-444.

Rentel, M.C., Leonelli, L., Dahlbeck, D., Zhao, B., and Staskawicz, B.J. (2008). Recognition of the *Hyaloperonospora parasitica* effector ATR13 triggers resistance against oomycete, bacterial, and viral pathogens. Proc Natl Acad Sci U S A **105,** 1091-1096.

Rocha, P.S., Sheikh, M., Melchiorre, R., Fagard, M., Boutet, S., Loach,

R., Moffatt, B., Wagner, C., Vaucheret, H., and Furner, I. (2005). The *Arabidopsis HOMOLOGY-DEPENDENT GENE SILENCING1* gene codes for an S-adenosyl-L-homocysteine hydrolase required for DNA methylation-dependent gene silencing. Plant Cell **17,** 404-417.

Sacco, M.A., Mansoor, S., and Moffett, P. (2007). A RanGAP protein physically interacts with the NB-LRR protein Rx, and is required for Rx-mediated viral resistance. Plant J **52,** 82-93.

Schulze-Lefert, P. (2004). Plant immunity: the origami of receptor activation. Curr Biol **14,** R22-24.

Sekine, K.T., Kawakami, S., Hase, S., Kubota, M., Ichinose, Y., Shah, J., Kang, H.G., Klessig, D.F., and Takahashi, H. (2008). High level expression of a virus resistance gene, *RCY1*, confers extreme resistance to *Cucumber mosaic virus* in *Arabidopsis thaliana*. Mol Plant Microbe Interact **21,** 1398-1407.

Seo, E., Kim, S., Yeom, S.I., and Choi, D. (2016). Genome-wide Comparative analyses reveal the dynamic evolution of nucleotide-binding leucine-rich repeat gene family among Solanaceae Plants. Front Plant Sci **7,** 1205.

Shen, Q.H., Zhou, F.S., Bieri, S., Haizel, T., Shirasu, K., and Schulze-Lefert, P. (2003). Recognition specificity and *RAR1/SGT1* dependence in barley *Mla* disease resistance genes to the powdery mildew fungus. Plant Cell **15,** 732-744.

Shen, Q.H., Saijo, Y., Mauch, S., Biskup, C., Bieri, S., Keller, B., Seki, H., Ulker, B., Somssich, I.E., and Schulze-Lefert, P. (2007). Nuclear activity of *MLA* immune receptors links isolate-specific and basal disease-resistance responses. Science **315,** 1098-1103.

Shibata, Y., Kawakita, K., and Takemoto, D. (2011). *SGT1* and *HSP90* are

essential for age-related non-host resistance of *Nicotiana benthamiana* against the oomycete pathogen *Phytophthora infestans*. Physiol Mol Biol Plants **75**, 120-128.

Shirasu, K. (2009). The HSP90-SGT1 chaperone complex for NLR immune sensors. Annu Rev Plant Biol, **60,** 139-164.

Slootweg, E.J., Spiridon, L.N., Roosien, J., Butterbach, P., Pomp, R., Westerhof, L., Wilbers, R., Bakker, E., Bakker, J., Petrescu, A.J., Smant, G., and Goverse, A. (2013). Structural determinants at the interface of the ARC2 and leucine-rich repeat domains control the activation of the plant immune receptors Rx1 and Gpa2. Plant Physiol **162,** 1510-1528.

Smadar harpaz-Saad, G.M.Y., Autar K. Tattoo, and Joseph J. Kieber. (2012). The formation of ACC and competition between polyamines and ethylene for SAM. Annu Plant Rev **44,** 53-81.

Stakman, E.C. (1915). Relation between *Puccinia graminis* and plants highly resistant to its attack. J Agric Res **4,** 193-199.

Sukarta, O.C.A., Slootweg, E.J., and Goverse, A. (2016). Structure-informed insights for NLR functioning in plant immunity. Semin Cell Dev Biol **56,** 134-149.

Swiderski, M.R., Birker, D., and Jones, J.D.G. (2009). The TIR domain of TIR-NB-LRR resistance proteins is a signaling domain involved in cell death induction. Mol Plant Microbe Interact **22,** 157-165.

Takken, F.L.W., Albrecht, M., and Tameling, W.I.L. (2006). Resistance proteins: molecular switches of plant defence. Curr Opin Plant Biol **9,** 383-390.

Tameling, W.I.L., Vossen, J.H., Albrecht, M., Lengauer, T., Berden, J.A.,

Haring, M.A., Cornelissen, B.J.C., and Takken, F.L.W. (2006). Mutations in the NB-ARC domain of I-2 that impair ATP hydrolysis cause autoactivation. Plant Physiol **140,** 1233-1245.

Tanaka, H., Masuta, C., Uehara, K., Kataoka, J., Koiwai, A., and Noma, M. (1997). Morphological changes and hypomethylation of DNA in transgenic tobacco expressing antisense RNA of the S-adenosyl-L-homocysteine hydrolase gene. Plant Mol Biol **35,** 981-986.

Tomita, R., Sekine, K.T., Mizumoto, H., Sakamoto, M., Murai, J., Kiba, A., Hikichi, Y., Suzuki, K., and Kobayashi, K. (2011). Genetic basis for the hierarchical interaction between *Tobamovirus* spp. and *L* resistance gene alleles from different pepper species. Mol Plant Microbe Interact **24,** 108-117.

Tornero, P., Gadea, J., Conejero, V., and Vera, P. (1997). Two *PR-1* genes from tomato are differentially regulated and reveal a novel mode of expression for a pathogenesis-related gene during the hypersensitive response and development. Mol Plant Microbe Interact **10,** 624-634.

Tran, D.T.N., Chung, E.H., Habring-Muller, A., Demar, M., Schwab, R., Dangl, J.L., Weigel, D., and Chae, E. (2017). Activation of a plant NLR complex through heteromeric association with an autoimmune risk variant of another NLR. Curr Biol **27,** 1148-1160.

van Hulten, M., Pelser, M., van Loon, L.C., Pieterse, C.M., and Ton, J. (2006). Costs and benefits of priming for defense in *Arabidopsis*. Proc Natl Acad Sci U S A **103,** 5602-5607.

Van Ooijen, G., Mayr, G., Kasiem, M.M.A., Albrecht, M., Cornelissen, B.J.C., and Takken, F.L.W. (2008). Structure-function analysis of the NB-ARC domain of plant disease resistance proteins. J Exp Bot **59,** 1383-1397.

Wang, G.F., Ji, J., El-Kasmi, F., Dangl, J.L., Johal, G., and Balint-Kurti, P.J. (2015). Molecular and functional analyses of a maize autoactive NB-LRR protein identify precise structural requirements for activity. PLoS Pathog **11,** e1004674.

Ward, H.M. (1902). On the relations between host and parasite in the Bromes and their Brown Rust, *Puccinia dispersa*. Ann Bot-London **16,** 233-315.

Weaver, L.M., Swiderski, M.R., Li, Y., and Jones, J.D.G. (2006). The *Arabidopsis thaliana* TIR-NB-LRR R-protein, RPP1A; protein localization and constitutive activation of defence by truncated alleles in tobacco and *Arabidopsis*. Plant J **47,** 829-840.

Weitzel, C., and Simonsen, H.T. (2015). Cytochrome P450-enzymes involved in the biosynthesis of mono- and sesquiterpenes. Phytochem Rev **14**, 7-24.

Williams, S.J., Sornaraj, P., deCourcy-Ireland, E., Menz, R.I., Kobe, B., Ellis, J.G., Dodds, P.N., and Anderson, P.A. (2011). An autoactive mutant of the M flax rust resistance protein has a preference for binding ATP, whereas wild-type M protein binds ADP. Mol Plant Microbe Interact **24,** 897-906.

Williams, S.J., Yin, L., Foley, G., Casey, L.W., Outram, M.A., Ericsson, D.J., Lu, J., Boden, M., Dry, I.B., and Kobe, B. (2016). Structure and function of the TIR domain from the grape NLR Protein RPV1. Front Plant Sci **7,** 1850.

Williams, S.J., Sohn, K.H., Wan, L., Bernoux, M., Sarris, P.F., Segonzac, C., Ve, T., Ma, Y., Saucet, S.B., Ericsson, D.J., Casey, L.W., Lonhienne, T., Winzor, D.J., Zhang, X.X., Coerdt, A., Parker, J.E., Dodds, P.N., Kobe, B., and Jones, J.D.G. (2014). Structural basis for

assembly and function of a heterodimeric plant immune receptor. Science **344,** 299-303.

Xiao, S., Ellwood, S., Calis, O., Patrick, E., Li, T., Coleman, M., and Turner, J.G. (2001). Broad-spectrum mildew resistance in *Arabidopsis thaliana* mediated by *RPW8*. Science **291,** 118-120.

Yoon, J., Chung, W.I., and Choi, D. (2009). *NbHB1*, *Nicotiana benthamiana* homeobox 1, is a jasmonic acid-dependent positive regulator of pathogen-induced plant cell death. New Phytol **184,** 71-84.

Zhang, X.X., Bernoux, M., Bentham, A.R., Newman, T.E., Ve, T., Casey, L.W., Raaymakers, T.M., Hu, J., Croll, T.I., Schreiber, K.J., Staskawicz, B.J., Anderson, P.A., Sohn, K.H., Williams, S.J., Dodds, P.N., and Kobe, B. (2017). Multiple functional self-association interfaces in plant TIR domains. Proc Natl Acad Sci U S A **114,** 2046-2052.

Zhang, Y., Dorey, S., Swiderski, M., and Jones, J.D. (2004). Expression of *RPS4* in tobacco induces an AvrRps4-independent HR that requires *EDS1, SGT1* and *HSP90*. Plant J **40,** 213-224.

Zhu, F., Xi, D.H., Yuan, S., Xu, F., Zhang, D.W., and Lin, H.H. (2014). Salicylic acid and jasmonic aid are essential for systemic resistance against *Tobacco mosaic virus* in *Nicotiana benthamiana*. Mol Plant Microbe Interact **27,** 567-577.

Zipfel, C. (2009). Early molecular events in PAMP-triggered immunity. Curr Opin Plant Biol **12,** 414-420.

ABSTRACT IN KOREAN

식물은 오랜 시간 동안 병원균에 대응해오면서 다양한 저항성 기작을 진화시켜 왔다. 그 중 nucleotide-binding domain and leucine-rich repeat (NLR) 유전자는 병원균이 식물에 병을 내기 위해 식물 세포 내로 분비하는 effector 단백질을 인지하여, 식물이 저항성 반응들을 나타낼 수 있도록 하는 대표적인 저항성 유전자이다. Effector 를 인지한 NLR 단백질은 구조 변화를 통해 활성 상태로 전환되고 그 이후 저항성 반응을 유도하게 하는데, 그 중 가장 강력한 저항성 반응으로 세포사멸(hypersensitive cell death)이 있다.

NLR 은 크게 3 개의 주요 도메인으로 구성되어 있다. C-말단에는 LRR 도메인, 중앙에는 NB-ARC 도메인, 그리고 N-말단에는 TIR 또는 CC 도메인이 존재한다. NLR 은 N-말단 도메인에 따라 TNL 과 CNL 로 나누어 진다. N-말단 도메인은 NLR 단백질의 신호를 전달하는 역할을 하며 병원균이 존재하지 않은 상황에서는 NB-ARC 또는 LRR 도메인과 상호작용을 통해 그 기능이 억제 되고 있다고 알려져 있다.

본 연구에서는 고추에 존재하는 NLR 유전자 415 개에 대하여 NLR 전체와 N-말단 도메인의 세포사멸활성을 Agrobacterium 을 이용한 일시적 과

발현을 통해 스크리닝하였다. 그 결과 그룹 10 번 NLR 의 CC 도메인이 특이적으로 높은 비율로 세포사멸활성을 가지는 것으로 확인되었다. 고추 외 다른 가지과 식물인 토마토와 담배의 그룹 10 번 NLR 의 CC 도메인도 세포사멸활성을 가지는 것으로 나타났다. 그룹 10 번 NLR 의 CC 도메인이 유도하는 세포사멸이 일어나는데 있어 NLR 의 molecular chaperone complex 가 필요하며, 세포사멸이 진행되는 동안 식물의 저항성반응에 관여하는 유전자들의 발현이 증가됨을 통해 그룹 10 번 NLR 의 CC 도메인의 과발현을 통해 유도된 세포사멸이 식물의 저항성 기작과 관련 있음을 입증하였다. 다음으로 그룹 10 번 NLR 의 CC 도메인이 유도하는 세포사멸에 관여하는 하위 신호전달 체계를 규명하기 위하여 VIGS 를 이용한 스크리닝을 진행하였다. NLR 타입 저항성 유전자가 매개하는 저항성의 중요 조절인자인 EDS1 과 NDR1, 그리고 SA 호르몬 생합성 및 하위 신호전달은 그룹 10 번 NLR 의 CC 도메인이 유도하는 세포사멸에 있어 필수적이지 않음을 밝혔다.

또한 그룹 10 번 NLR 의 CC 도메인들의 구조 분석을 통한 기능 연구를 통해 CC 도메인의 첫번째 α-helix 가 세포사멸활성에 중요함을 확인하였다. 그룹 10 번 NLR 의 CC 도메인의 세포사멸 기작을 이해하기 위하여 CC 도메인의 상호작용인자를 동정하기 위한 pull-down 및 LC-MS/MS 실험을 진행한 결과 S-adenosyl homocysteine hydrolase (SAHH) 가 CC 도메인의

상호작용 후보 유전자로 동정되었다. SAHH는 CC 도메인과 동시 과발현시 CC 도메인이 유도하는 세포사멸을 억제하는 것으로 보아 CC 도메인의 세포사멸활성의 negative regulator 로서의 역할을 하는 것으로 추측된다. SAHH 유전자의 발현이 감소한 담배식물체에서는 병원균 접종 없이도 ROS가 과다 축적되었고, 이를 통해 CC 도메인이 SAHH를 비활성화 시킴으로써 ROS가 증가되어 세포사멸을 유도하는 것으로 유추할 수 있었다.

본 연구를 통해 그룹 10번 NLR의 CC 도메인이 특이적으로 세포사멸을 유도한다는 것이 밝혀졌다. 그룹 10번 NLR의 CC 도메인이 유도하는 세포사멸기작에 대한 연구는 NLR 단백질이 어떻게 세포사멸을 유도하는지, 더 나아가 식물의 병 저항성에 있어 고추의 그룹 10번 NLR 유전자들의 기능에 대한 이해를 돕는 데 실마리가 될 것이다.